UNIVERSIDAD
NACIONAL
DE COLOMBIA

Influence of tree-level and species-level factors on the mortality of canopy trees in an Amazon forest: linking remote sensing with ground-based data

Luisa Fernanda Gómez Correa

Universidad Nacional de Colombia

Facultad de Ciencias Agrarias, Departamento de Ciencias Forestales

Medellín, Colombia

2022

Influence of tree-level and species-level factors on the mortality of canopy trees in an Amazon forest: linking remote sensing with ground-based data

Luisa Fernanda Gómez Correa

Tesis presentada como requisito parcial para optar al título de:

Magíster en Bosques y Conservación Ambiental

Director:

Ph.D. Álvaro Javier Duque Montoya

Codirector:

Ph.D. Daniel Felipe Zuleta Zapata

Línea de Investigación:

Ecología de Ecosistemas Terrestres

Grupo de Investigación:

Conservación, Uso y Biodiversidad

Universidad Nacional de Colombia

Facultad de Ciencias Agrarias, Departamento de Ciencias Forestales

Medellín, Colombia

2022

A todas y todos aquellos que defienden el medio ambiente y su territorio. Para aquellos que no sabemos dónde están o a quienes les arrebarataron la vida por querer un mundo mejor.

Construyamos un mundo con espacio para todos, empezando siempre por cambiarnos a nosotros mismos.

To all those who defend the environment and their territory. To those who we don't know where they are or those who their lives were taken just for wanting a better world.

Let's build a world with space for everyone, always starting by changing ourselves.

Declaración de obra original

Yo declaro lo siguiente:

He leído el Acuerdo 035 de 2003 del Consejo Académico de la Universidad Nacional. «Reglamento sobre propiedad intelectual» y la Normatividad Nacional relacionada al respeto de los derechos de autor. Esta disertación representa mi trabajo original, excepto donde he reconocido las ideas, las palabras, o materiales de otros autores.

Cuando se han presentado ideas o palabras de otros autores en esta disertación, he realizado su respectivo reconocimiento aplicando correctamente los esquemas de citas y referencias bibliográficas en el estilo requerido.

He obtenido el permiso del autor o editor para incluir cualquier material con derechos de autor (por ejemplo, tablas, figuras, instrumentos de encuesta o grandes porciones de texto).

Por último, he sometido esta disertación a la herramienta de integridad académica, definida por la universidad.

_____

Luisa Fernanda Gómez Correa

Fecha 21/06/2022

Acknowledgements

I want to express my gratitude to my advisor Prof. Álvaro Duque, for all the trust, the patience, and for guiding me in the research path. I am very grateful to my co-advisor Daniel Zuleta, who has guided me all this way, with a lot of listening, enthusiasm, and a contagious motivation. Daniel is a role model, not only in the professional and academic aspect but also as the good person he is.

I would like to thank my parents, my brother, and my sister-in-law, who has supported me throughout this process. To Juan Pablo Henao, Paola Jaramillo, Mariana Gutiérrez, Natali Caro, and Maria Camila Jaramillo, who had supported me and cared about my research project.

This work was made possible by Parques Nacionales Naturales de Colombia and the Instituto Amazónico para Investigaciones Científicas SINCHI. Special thanks to Eliana Martinez and the crew of the Amacayacu Natural National Park, for the facilities in the field and for their kindness. I also want to express my gratitude to Dairon Cárdenas; he did so much for Amazon forests including Amacayacu, that very little of this would have been possible without his great contribution. I am grateful for the great assistance of coworkers of the indigenous community of Palmeras and for all the students of forest engineering from Universidad Nacional de Colombia, who had put their time and energy into investigating this wonderful ecosystem. I specially thank to Maria Camila Jaramillo who worked with me on this project, Jörg Haarpaintner and Fabian Enßle with the canopy orthomosaic, Santiago Múnera with field check, Mariana Gutierrez with crown survey, and Raquel F. Araujo and Gabriel Arellano with valuable comments and help.

I was supported by MinCiencias “Convocatoria 891 2020 Jóvenes Investigadores”.

This work would not have been possible without the support of the Forest Global Earth Observatory (ForestGEO) of the Smithsonian Tropical Research Institute for partial support of the plot censuses and field training provided to hundreds of students in Amacayacu.

Resumen

Influencia de los factores de individuo y especie en la mortalidad de los árboles de dosel en un bosque de la Amazonía: vinculación de sensores remotos y datos terrestres

La mortalidad de los árboles es un proceso ecológico fundamental que determina la estructura y funcionamiento de los bosques. En este estudio, vinculamos datos de sensores remotos y monitoreos terrestres para evaluar la influencia de la exposición de la copa de los árboles a la luz (en relación con el área total de la copa), la desviación individual de las tasas de crecimiento, el tamaño del árbol (DBH), y la densidad de la madera de las especies, sobre la mortalidad de 984 árboles de dosel en la Parcela Permanente Amacayacu, Amazonía noroccidental, entre el 2013 y 2019. Ajustamos Modelos Lineales Generalizados de Efectos Mixtos para investigar las variables o combinación de variables que mejor explicaba la probabilidad de muerte durante este período. Encontramos que los árboles de dosel de especies con baja densidad de la madera fueron menos propensos a morir cuando tuvieron mayor proporción de copa expuesta a la luz, mientras que, árboles de alta densidad de madera fueron ligeramente más propensos a morir a mayor proporción de su copa expuesta a la luz. Árboles que crecieron menos que el promedio de su especie presentaron mayor mortalidad, especialmente en especies con baja densidad de la madera. El rol de la densidad de la madera en la determinación de la sobrevivencia de los árboles de dosel bajo diferentes condiciones de luz indica respuestas diferenciales de las estrategias de historia de vida. Nuestros resultados destacan la importancia de tener en cuenta las estrategias de historia de vida (e.g., representadas por la densidad de la madera) al predecir la demografía de los bosques bajo el rápido cambio climático.

Palabras clave: área de copa; densidad de la madera; disponibilidad de luz; drones; estrategias de historia de vida; sobrevivencia arbórea; tasas de crecimiento; tamaño del árbol.

Abstract

Influence of tree-level and species-level factors on the mortality of canopy trees in an Amazon forest: linking remote sensing with ground-based data

Tree mortality is a fundamental ecological process determining forest structure and functioning. Here, we linked remote sensing and ground-based data to assess the influence of tree crown exposure to light (relative to total crown area), individual deviations of growth rates, tree size (DBH), and species wood density on the mortality of 984 canopy trees for the Amacayacu Forest Dynamics Plot, northwestern Amazon, between 2013 and 2019. We fitted Generalized Linear Mixed-Effects models to investigate the variables or combination of variables that best explained the probability of death during this period. We found that canopy trees of low wood density species were less prone to die when their proportion of crown was more exposed to sunlight, whereas high wood density trees were slightly more prone to die with higher relative crown exposure to light. Trees growing less than their species average had higher mortality, especially in low wood density species. The role of wood density in determining the survival of canopy trees under varying light conditions indicates differential responses of life-history strategies. Our results highlight the importance of accounting for life-history strategies (e.g., proxied by wood density) when predicting forest demography under rapidly changing climate.

Keywords: crown area; drones; growth rates; life-history strategies; light availability; tree size; tree survival; wood density.

Content

List of figures

Page.

List of tables

Page.

List of supporting information

Page.

Page.

Introduction

Tree mortality highly influences forest carbon dynamics, functioning, and composition. Increases in tree mortality have been proposed to be the main cause of the long-term decline in Amazon carbon stocks (Hubau *et al.*, 2020) with negative consequences for the global climate regulation (Friedlingstein *et al.*, 2022). However, what drives changes in tree mortality as well as the covariates influencing trees' response remain poorly understood (McDowell *et al.*, 2022), especially in the tropics, where the high species diversity results in multiple responses to a given factor (Zuleta *et al.*, 2022a; Bauman *et al.*, 2022). The multivariate nature of tree mortality and the relatively low numbers of trees dying every year make it a difficult process to understand, estimate, and ultimately predict (McMahon *et al.*, 2019).

Tree mortality results from a combination of factors (Franklin *et al.*, 1987). Some of these are slow or chronic factors (e.g., genetic factors, resource limitation; 'presses', Harris *et al.,* 2018), while others can kill trees within a single season (e.g., drought, pest outbreak) or almost instantaneously (e.g., lightning, wind disturbances; 'pulses', Negrón-Juárez *et al.*, 2017; Yanoviak *et al.*, 2020). These factors are non-mutually exclusive and operate at the individual, species, and stand levels (e.g., Arellano *et al.*, 2019; Aleixo *et al.*, 2019; Esquivel-Muelbert *et al.*, 2020). At the species level, trees generally array on a continuum of resource allocation strategies (i.e., the growth-mortality trade off; Wright *et al.,* 2010) with fast-growing species dying faster than slow-growing species, especially in undisturbed tropical forests (Russo *et al.*, 2021). The low mortality of slow growing species is presumably mediated by their high wood density, a key trait that provides mechanical support, hydraulic safety during droughts, and greater resistance to pests and pathogens (Augspurger & Kelly, 1984; Hacke *et al.*, 2001; Chave *et al.*, 2009). Within species, however, trees that grow faster than conspecifics have greater access to resources and therefore are less prone to die (Rüger *et al.*, 2011; Camac *et al.*, 2018; Arellano *et al.*, 2019; Russo *et al.*, 2021).

Resource availability, both aboveground and belowground, also influences tree mortality (Russo *et al.*, 2005; Zuleta *et al.*, 2017; Arellano *et al.*, 2019). Light limitation has been found to be one of the most prevalent and impactful mortality risks in six tropical forests, even for trees larger than 10 cm in diameter (Zuleta *et al.*, 2022a). Light, as the fundamental source of energy for photosynthesis, constitutes one of the major resources for which trees compete (Wright, 2002). Light-limited trees are more prone to die by competition (Muller-Landau *et al.*, 2006), but also by other comorbidity factors such as falling branches/trunks of neighboring trees (Zuleta *et al.*, 2022a). However, large trees can also be more likely to die because they are subjected to high evaporative demands, high winds, lightning, and have accumulated more damage by living longer (Bennett *et al.*, 2015; Yanoviak *et al.*, 2020; Gora & Esquivel-Muelbert, 2021). It is common in tropical forests that intermediate size trees die less than both small and large trees (Rüger *et al.*, 2011; Arellano *et al.*, 2019).

The canopy forest layer is highly diverse and is mainly composed of large-sized trees that contribute most to biomass and woody productivity (Lutz *et al.*, 2018; Araujo *et al.*, 2020; Piponiot *et al.*, 2022). Large trees are particularly vulnerable to water stress, wind and lighting and these abiotic drivers are predicted to increase with global warming (Gora & Esquivel-Muelbert, 2021; McDowell *et al.*, 2022). The survival of canopy trees in Amazon *terra firme* forests have been found to be strongly driven by extreme climatic events, wood density, successional position, and deciduousness; where soft-wooded, pioneer, and evergreen species are particularly vulnerable to extreme years (Aleixo *et al.*, 2019). Overall, tree mortality is projected to increase with climate change (Bauman *et al.*, 2022; McDowell *et al.*, 2022) where large trees will have a disproportionately impact on carbon stocks. However, focused investigations are needed to understand how tree- and species-level factors could influence tree survival.

Recent studies have used remote sensing to evaluate the linkages of tree mortality with abiotic factors (e.g., precipitation, soil characteristics; Araujo *et al.*, 2021; Cushman *et al.*, 2022). High resolution images, such as those obtained with Remotely Piloted Aircraft Systems (RPAS, also known as drones), are a remote sensing product that allows to get attributes on difficult to sample locations, such as the canopy forest layer. Moreover, the integration of remote sensing with ground-based data allows to broaden the perspective of ecological processes as is tree mortality.

Here, we assessed the influence of tree- and species-level factors on the mortality of canopy trees in the Amacayacu Forest Dynamics Plot in Colombia, northwestern Amazon. We used an orthomosaic derived from a RPAS, and two censuses of the 25-ha plot to evaluate the role of crown exposure to light (relative to total crown area), individual deviations of growth rates, tree size (DBH), and species wood density on the survival of canopy trees between 2013 and 2019. We asked: What are the tree- and species-level factors that influenced canopy tree mortality during this period? Given the importance of light in plant processes, we expect trees with higher proportions of their crown exposed to direct sunlight to die less compared to less sun-exposed trees. We also expect this effect to covary with tree size, growth rates, and the species wood density, due to the different life history strategies.

1. Materials and methods

1.1 Study area

This study was carried out at the 25 ha Amacayacu Forest Dynamics Plot (AFDP), located in the Amacayacu National Natural Park in Colombia (3°48'33.02" S and 70°16'04.29" W), northwestern Amazon. The AFDP is located on a highly-diverse *terra firme* forest (Duque *et al.*, 2017) and is part of the Forest Global Earth Observatory (ForestGEO; Davies *et al.* 2021). The mean annual temperature is 25.8°C, mean annual precipitation is 3,216 mm and mean relative humidity is 86% (Zuleta *et al.*, 2020).The plot is located on tertiary sediments of Pebas geological formation, the elevation varies between 89 and 108 m.a.s.l with hilly and moderately dissected topography, and has poor soils, high acidity, and low base saturations due to the dominance of minerals such as kaolinite and quartz (Chamorro, 1989; Zuleta *et al.*, 2020). The AFDP has 579 ± 38 individuals per ha with diameter at breast height (DBH) ≥ 10 cm, with a total of 642 named species at the 25 ha (Duque *et al.*, 2017). The canopy layer is situated approximately above 25 m of altitude.

1.2 Data collection and processing

We tested the role of species-adjusted tree growth rates (SA-GR), tree size (log(DBH)), relative crown exposure to light (RCEL), and species wood density (WD) on the mortality of 984 canopy trees of 265 species (48 families) in the AFDP. We gathered these variables for each tree in 2013 and assessed their survival status in 2019. Below, we described the methods to obtain each of these variables.

1.2.1 Forest censuses

The AFDP was established between April 2007 and December 2009, where all free-standing woody stems (i.e., trees, shrubs, palms and tree ferns) with DBH ≥ 1 cm were mapped, tagged, measured, and collected for species identification. The second and third

censuses were carried out between October 2013 and March 2016 and between July 2019 and February 2022, respectively. During these full censuses the survival of all trees were assessed, the DBH for surviving trees was recorded, and all new recruits were measured, tagged, mapped, and identified. The mean census intervals between the first and second census (2007-2013) and between the second and third census (2013-2019) were 6.7 (standard deviation (SD) =1.1) and 5.2 (SD=1.3) years, respectively. Voucher specimens were deposited and identified in the Herbario Amazónico Colombiano (COAH) of the Instituto Amazónico de Investigaciones Científicas SINCHI.

1.2.2 Species-adjusted tree growth rates (SA-GR)

To estimate the tree growth rate deviation from the species average (SA-GR), we calculated growth rates (g, cm yr^{-1}) of trees with DBH ≥ 1 cm across the two census intervals (from 2007 to 2013 and from 2013 to 2019) in the 25 ha of the AFDP as:

$$g = \frac{DBH_{final} - DBH_{initial}}{time_{final} - time_{initial}},$$

where $DBH_{initial}$ and DBH_{final} are the diameters at the breast height (cm) at $time_{initial}$ and $time_{final}$, respectively, for each census interval. If the diameters were not measured at 1.3 m height we calculated the corrected DBH using the following taper equation (Metcalf *et al.*, 2009):

$$DBH_{corrected} = D^{\alpha(HOM - 1.3)},$$

Where α is the tapering factor and HOM is the height (m) of measurement of diameter D (cm). The tapering factor α was estimated for each tree as (Cushman *et al.*, 2021):

$$\alpha = 0.151 - 0.025 \times \log(D) - 0.02 \times \log(HOM) - 0.021 \times \log(WD) + site,$$

where WD is the wood density of the species (g cm^{-3}) and $site$ takes the value of -0.00161 for the AFDP.

We assumed as errors and therefore excluded tree measurements in which the DBH_{final} was > $4SD$ below the $DBH_{initial}$ (Condit *et al.*, 2004), where:

$$SD = (0.006214 \times DBH_{initial}) + 0.9036$$

We also excluded trees with g > 4 cm yr^{-1}. Since the distribution of g is extremely right-skewed, we applied the modulus transformation on the growth rates, which reduces the

skewness of the data and allows the inclusion of negative growth rates (Condit *et al.*, 2017). The modulus-transformed growth rate (GR) was calculated as:

$$GR(\theta) = \begin{cases} g^{\theta} & g \geq 0 \\ -\{(-g)^{\theta}\} & g < 0 \end{cases}$$

We used a $\theta = 0.4$ since this value minimized the skewness of the growth rates of trees in the AFDP across both census intervals (Figure S1, Figure S2, Figure S3). We used GR instead of relative growth rates because the latter depends on tree size (Figure S4).

Finally, we estimated the SA-GR (unitless) for each tree *i* of species *j* in our sample (i.e., crown delimited trees) as:

$$Species\ adjusted\ GR_{i,j} = \frac{GR_{i,j} - mean(GR)_j}{standard\ deviation\ (GR)_j}.$$

We limited our analysis to species with at least 25 growth observations to avoid unreliable estimates due to lack of variability in rare species.

1.2.3 Tree size (log(DBH))

To estimate the effect of tree size on mortality, we calculated the corresponding DBH (cm) of each tree at the time of the RPAS flight as:

$$DBH_{flight} = DBH_{2007} + \left[g \times (time_{flight} - time_{2007})\right],$$

where DBH_{2007} is the DBH (cm) of the tree at $time_{2007}$ (first full census), g is its growth rate (cm yr^{-1}), and $time_{flight}$ is the date of the RPAS flight. This DBH was finally log-transformed to improve model fitting.

1.2.4 Relative crown exposure to light (RCEL)

To assess the influence of light availability on canopy tree mortality we derived an unitless metric calculated as (Figure 1-1):

$$RCEL = \frac{ECA}{CA},$$

where ECA is the vertically sun-exposed crown area (m^2), calculated from a canopy orthomosaic obtained from a remotely piloted aircraft system (RPAS) (*see below*); and CA is the total crown area (m^2) estimated from an allometric model based on DBH_{flight} (*see below*). RCEL indicates the proportion of total DBH-derived crown area of a tree that is exposed to vertical sunlight and, thus, varies from 0 to 1. Trees with RCEL values close to

1 are more exposed to vertical sunlight, whereas trees with RCEL values close to 0 are less exposed to sunlight. We excluded trees with an ECA greater than the upper confidence interval of the prediction of crown area (five trees) and truncated to RCEL = 1 those trees with RCEL > 1 (70 trees). Note that, ecologically, this metric cannot distinguish between the processes driving the actual crown area, therefore, trees with RCEL < 1 might either be shaded by other trees or have an incomplete crown due to damage or other factors. Overall, RCEL is a measure of resource acquisition relative to the potential resource acquisition for a tree of a given size, a proxy for the “payback” or “return” on the resource investment for any given tree.

1.2.5 Vertically sun-exposed crown area (ECA)

Near-infrared (NIR) images of the AFDP canopy were obtained using a RPAS in December 2013, during the 9th Regional SilvaCarbon/GFOI Workshop on Forest Monitoring. This flight was made right at the beginning of the second census and aimed to characterize the conditions of canopy trees around the date in which trees were measured on the ground. The researchers used a fixed-wing SenseFLY Ebee integrated with a camera Canon PowerShot ELPH 110 HS with 4.3 mm focal length and 16 mpx of photo resolution. The total number of photos taken were 264 and the flying altitude was 112 m. They processed the photos on the photogrammetry software Agisoft Photoscan (https://www.agisoft.com, v.0.9.1) and generated a 6 cm spatial resolution orthomosaic. The georeferencing accuracy was assessed in terms of the root mean square error, where the X, Y, and Z errors were 1.8, 0.7, and 13.5 m, respectively. The orthomosaic reproduces the real dimensions of tree crowns.

We delimited all identifiable crowns of living trees with DBH ≥ 10 cm based on the NIR image and assigned their corresponding tag (i.e., unique individual code of the plot) over 18 ha of the AFDP using QGIS software v.3.16.5 (QGIS Geographic Information System, 2022). We carried out a semi-automated crown delimitation in which we first segmented the orthomosaic into polygons using the *segmentation* function of Orfeo ToolBox (Grizonnet *et al.*, 2017) with a minimum region size of 7000 pixels (25.2 m^2) and then, manually edited these polygons to adjust them to the actual tree crowns. For each 20 m x 20 m plot

quadrant, we first assigned and adjusted tree crowns for individuals with the biggest DBHs followed by the consecutively smaller DBHs because the probability of being in the canopy increases logistically with diameter (Araujo *et al.*, 2020). Finally, we carried out a ground validation of the crown-tag assignments on the field for a random sample of 3% of the total number of trees initially delimited as well as for trees that were classified as unreliable during the crown delimitation process. We calculated ECA (m^2) as the polygon area of each crown-delimited tree.

1.2.6 Total crown area (CA)

We estimated the CA (m^2) of each crown-delimited tree at the time of the RPAS flight based on an allometric model constructed from a crown survey for 622 trees of 148 species in the AFDP. In this crown survey, we measured the DBH and the four radii of the crown of each tree (*sensu* Bohlman & O'Brien, 2006). We calculated the crown area based on the four radii assuming circular crowns and excluded heavily damaged trees. We fitted a Linear Mixed-Effects Model (LMM) of total crown area as a function of DBH following a power function (i.e., $CA = aDBH^b$), and included species (s) random intercepts and slopes to account for differences in tree architecture (Martínez-Cano *et al.*, 2019; Zuleta *et al.*, 2022b) (Table S1**;** Figure S5). In *lme4* R notation, the formula was log(CA) ≈ 1+ log(DBH) + (1 + *s* | *s*). We evaluated the model residuals following a simulation-based approach (Figure S6). The total crown area for each of the crown-delimited trees was obtained from the predictions of this model based on the DBH_{flight} and their species identity. Species-specific random parameters were used if the species was present in the crown survey (78 species), whereas parameters from the averaged-population model were used if the species was not in the crown survey (187 species). We multiplied the model predictions by $\exp(RSE^2/2)$ to correct the bias introduced by back transforming predictions of log-scale models (RSE: residual standard error of the fitted model).

Figure 1-1. Outline of methodology to estimate the Relative Crown Exposure to Light (RCEL) of canopy trees in the Amacayacu Forest Dynamics Plot (AFDP), northwestern Amazon. (a) The vertically sun-Exposed Crown Area (ECA, green polygons) of 984 trees of 265 species (48 families) was estimated using a near-infrared orthomosaic of the canopy of the AFDP. (b) Detailed ECA delimitation with the corresponding tree tag. (c) Ground-based Crown Area (CA) survey for 622 trees of 148 species at the AFDP, where the DBH

and four radii of the crown of each tree were measured. (d) The CA survey was used to construct a Linear Mixed-Effects Model (LMM) to predict total CA as a function of DBH following a power function with species random intercepts and slopes. (e) Representation of the vertically sun-exposed crown area (ECA) and the total crown area (CA) to estimate (f) the relative crown exposure to light (RCEL) of a given tree. In (a) and (b) green polygons correspond to the vertically sun-exposed crown boundaries of each tree (i.e., observed from above) and black lines indicate 20 m x 20 m quadrats. This study was restricted to 18 out of 25 ha for which the survival of trees was assessed prior to the COVID-19 Pandemic. Figure S7 shows the status of these canopy trees (alive or dead) in 2019.

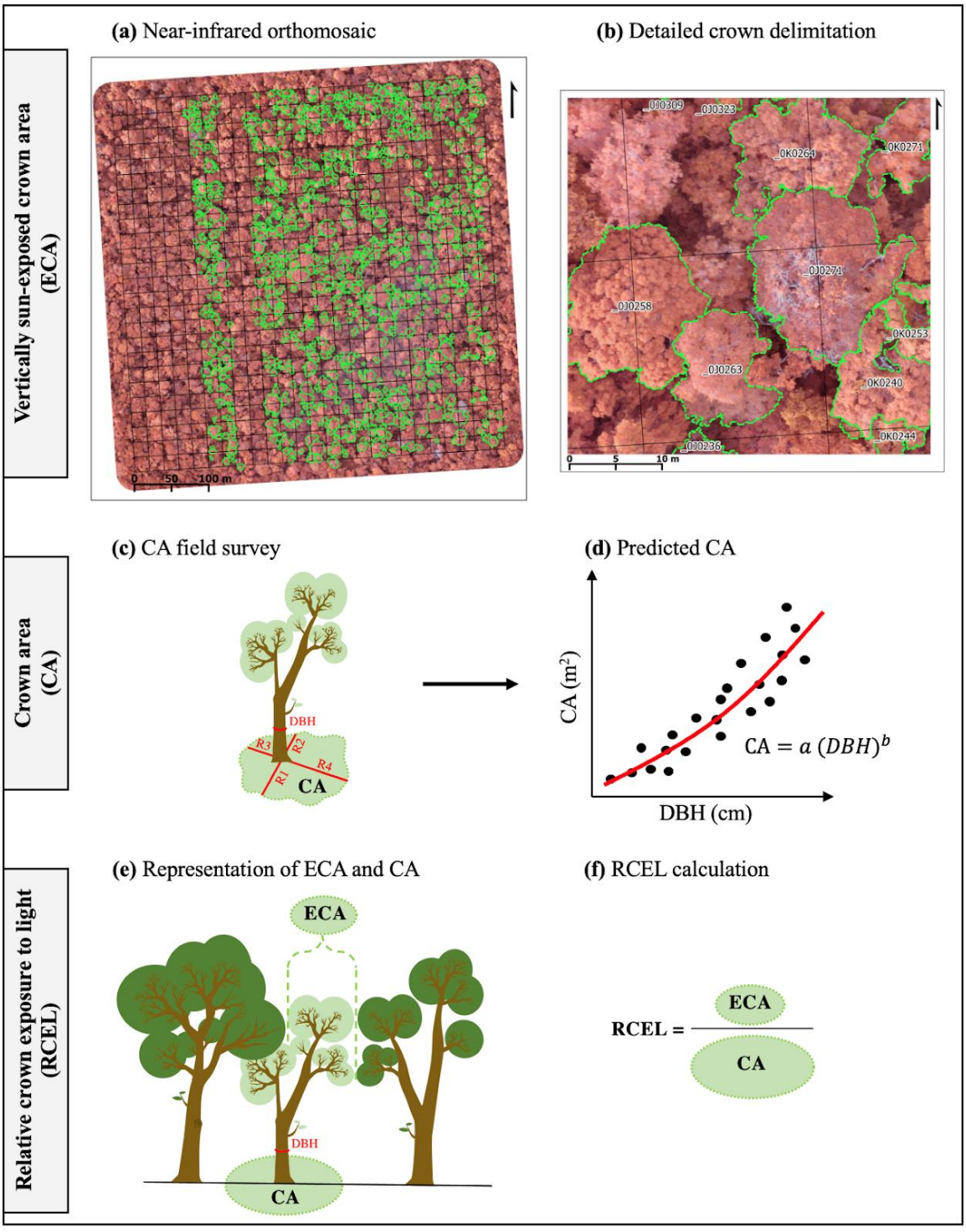
(a) Near-infrared orthomosaic
(b) Detailed crown delimitation
Vertically sun-exposed crown area (ECA)
0 50 100 m
0J0309
0J0323
0K0264
0K0271
0J0271
0J0258
0K0253
0J0263
0K0240
0K0244
0J0236
0 5 10 m
(c) CA field survey
(d) Predicted CA
Crown area (CA)
DBH
R1
R2
R3
R4
CA
CA (m²)
CA = a (DBH)^b
DBH (cm)
(e) Representation of ECA and CA
(f) RCEL calculation
Relative crown exposure to light (RCEL)
ECA
DBH
CA
RCEL = ECA / CA

1.2.7 Species wood density (WD)

We obtained WD (g cm^{-3}) for each species according to literature (Chave *et al.*, 2006; Zanne *et al.*, 2009), giving priority to data nearest to the AFDP. When species-level values were not available we used genus-level, family-level, or the site average (Chave *et al.*, 2006).

1.2.8 Tree mortality rates

For descriptive purposes, we calculated the annual mortality rate (λ, % yr^{-1}) of canopy trees between the date of the RPAS flight and the third census as:

$$\lambda = \frac{\log\left(N_{flight}\right) - \log\left(S_{2019}\right)}{time_{2019} - time_{flight}},$$

where N_{flight} is the number of trees alive at $time_{flight}$ (second census) and S_{2019} is the number of those trees that survived until $time_{2019}$ (third census).

1.3 Model fitting

To assess the influence of relative crown exposure to light, species-adjusted tree growth rates, tree size and species wood density on the mortality of canopy trees in the AFDP, we investigated the variables or combination of variables that best explained the probability of death using Generalized Linear Mixed-Effects Models (GLMM, logit link) including species random intercepts. We fitted 16 GLMMs with all possible combinations of covariates and their second-order interactions, including the full (all covariates) and the null (i.e., only intercept) models. We calculated their second-order Akaike's information criterion (AICc) using the *AICcmodavg* package (Mazerolle, 2020). We ranked the models and selected the one with the lowest AICc as the best model (Burnham & Anderson, 2002). We also considered the inclusion of the log-transformed exposed crown area (log(ECA)) and the modulus-transformed tree growth rate (GR) as covariates but they were removed during preliminary analysis due to their high collinearity with other variables (Table S2).

Mixed-effects models were fitted by maximum likelihood estimation (Laplace approximation) using the *lme4* R package (Bates *et al.*, 2015). Model residuals were evaluated with the *DHARMa* R package (Hartig, 2021). Conditional (R^2C) and marginal

coefficients (R^2M) of determination were calculated with the *MuMIn* R package (Barton, 2022). All analyses were performed in R v.4.0.4 (R Core Team, 2021).

2. Results

Of the 984 canopy trees in our sample, we recorded 101 dead trees (10.3%) after a mean period of 6 (SD=0.2) years, which corresponded to an annual mortality rate of 1.82% yr^{-1}. Dead canopy trees died all over the 18 ha sampled in the AFDP (Figure S7). Trees in our sample covered a wide range of diameters (10.73 – 138.84 cm, DBH), crown areas (21.54 – 473.72 m^2, CA), sun-exposed crown areas (2.45 – 460.87 m^2, ECA), species-adjusted growth rates (-4.19 – 4.25, SA-GR), and species' wood densities (0.20 – 1.05 g cm^{-3}, WD) (Table S3; Figure S8).

The mortality model with the lowest AICc included RCEL, WD, SA-GR, and their second-order interactions (Table 2-1). The main effects of these variables and the interaction between RCEL and WD were highly significant (Table S4). Our model was correctly specified according to residual diagnostics (Figure S9), and there was no evidence of spatial autocorrelation in the probability of death (Figure S10) or in the residuals of the model (Figure S11). Overall, the probability of death decreased with WD, trees with the lowest WD had an estimated 12% probability of dying after the 6 years, while trees with the highest WD had three times lower probability of dying (4%) after that time period (Figure 2-1a). The SA-GR was negatively related to the probability of death. Trees growing at the same rate as their species average (SA-GR=0) had 9% probability of dying after the 6 years, whereas trees with the highest growth compared to their species average had three times lower probability of dying (3%) (Figure 2-1b).

The total effect of RCEL on the probability of death was virtually constant, both the least sun-exposed trees (RCEL = 0.04) and totally sun-exposed trees (RCEL = 1) had 8% probability of dying after the 6 years (Figure 2-1c). However, the effect of RCEL was particularly influenced by their interactions with WD and SA-GR (Table 2-1;Table S4). RCEL was negatively related to mortality for trees belonging to species with low WD (≤ 0.47 g cm^{-3}) (Figure 2-2a), but positively related to mortality for trees with high WD (> 0.77 g cm^{-}

^{3}) (Figure 2-2c). Trees with intermediate WD (0.47 g cm^{-3} < WD ≤ 0.77 g cm^{-3}) had relatively constant probability of death across RCEL values (Figure 2-2b; Figure S12a). The effect of SA-GR on the probability of death was consistently negative for trees with low and intermediate WD, but not for trees with high WD (Figure 2-2 ;Figure S12b). Overall, high probabilities of death were predicted for trees with low RCEL, low WD, and low SA-GR simultaneously.

Table 2-1: Comparison of the 16 Generalized Linear Mixed-Effects Models to predict canopy tree mortality (M) using tree- and species-level factors. Models are ranked according to the difference in Akaike information criterion value corrected for small samples (ΔAICc) compared to the best model. Candidate fixed effects were relative crown exposure to light (RCEL, unitless), log-transformed size (log(DBH), cm), wood density (WD, g cm^{-3}) and species-adjusted growth rate (SA-GR, unitless). All models included species as random intercept and second-order interactions among the fixed effects (not shown on the model description). Marginal (R^2M) and conditional (R^2C) R^2 are the amount of variation explained by fixed effects and combined fixed + random effects, respectively (Nakagawa & Schielzeth, 2013). Total number of parameters (K), root mean squared error (RMSE) and log-likelihood (LL) are given for each model.

Model	**K**	**R^2M**	**R^2C**	**RMSE**	**LL**	**AICc**	**ΔAICc**
M ~ RCEL + WD + SA-GR	8	0.06	0.23	0.28	-307.61	631.38	0.00
M ~ WD + log(DBH) + SA-GR	8	0.07	0.21	0.28	-308.67	633.50	2.12
M ~ RCEL + WD + log(DBH) + SA-GR (full model)	12	0.09	0.26	0.28	-304.86	634.04	2.67
M ~ WD + SA-GR	5	0.04	0.18	0.29	-313.36	636.78	5.40
M ~ RCEL + WD	5	0.04	0.23	0.28	-313.45	636.96	5.58
M ~ RCEL + WD + log(DBH)	8	0.06	0.26	0.28	-310.61	637.38	6.00
M ~ RCEL + SA-GR	5	0.03	0.21	0.28	-314.24	638.54	7.17
M ~ SA-GR	3	0.02	0.19	0.29	-316.32	638.66	7.28
M ~ WD + log(DBH)	5	0.05	0.20	0.29	-314.59	639.24	7.87
M ~ log(DBH) + SA-GR	5	0.03	0.20	0.28	-314.62	639.30	7.92
M ~ RCEL + log(DBH) + SA-GR	8	0.04	0.23	0.28	-312.59	641.32	9.94
M ~ WD	3	0.01	0.17	0.29	-318.24	642.50	11.12
M ~ log(DBH)	3	0.01	0.18	0.29	-318.29	642.61	11.23
M ~ 1 (null model)	2	0.00	0.17	0.29	-319.51	643.03	11.65

Model	K	R^2M	R^2C	RMSE	LL	AICc	ΔAICc
M ~ RCEL	3	0.00	0.19	0.28	-319.02	644.06	12.68
M ~ RCEL + log(DBH)	5	0.02	0.22	0.28	-317.06	644.18	12.80

Figure 2-1: Predicted probability of death (%) for canopy trees in the Amacayacu Forest Dynamics Plot as a function of (a) wood density (WD, g cm^{-3}), (b) species-adjusted growth rate (SA-GR, unitless), and (c) relative crown exposure to light (RCEL, unitless). Lines represent the adjusted predictions from the model for each variable leaving the others conditioned at their mean and shaded areas indicate the 95% confidence interval. Point sizes are scaled according to the DBH of the trees. The second vertical axis, λ, shows the corresponding annual mortality rate (% yr^{-1}) for the predicted probability of death in a 6-year period. The color of the points in (b) and (c) indicates WD classes.

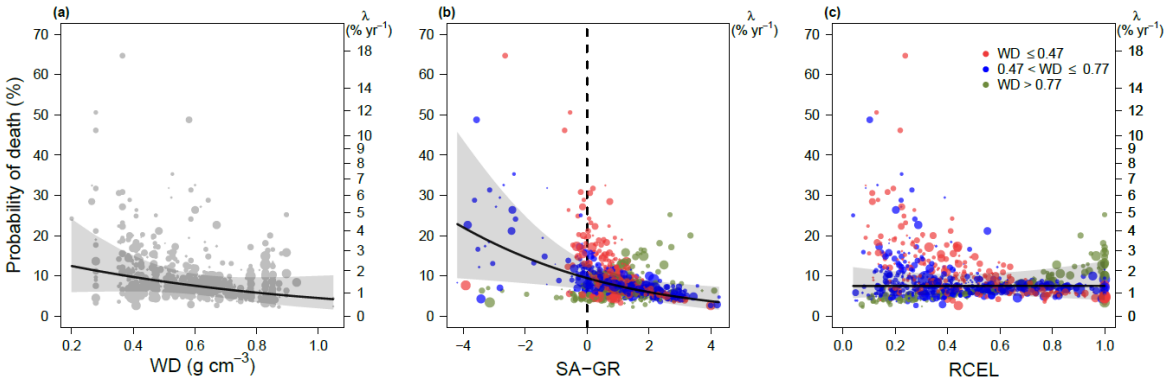

Figure 2-2: Predicted probability of death (%) for canopy trees in the Amacayacu Forest Dynamics Plot as a function of relative crown exposure to light (RCEL, unitless) for three classes of wood density (WD, panels) within three classes of species-adjusted growth rate (SA-GR, color points). Lines represent the adjusted predictions from the model conditioned to reference values and shaded areas indicate the 95% confidence interval. Point sizes are scaled according to the DBH of the trees. The second vertical axis, λ, shows the corresponding annual mortality rate (% yr^{-1}) for the predicted probability of death in a 6-year period. Reference values were adjusted for WD at 0.41 g cm^{-3} in (a), 0.60 g cm^{-3} in (b) and

0.83 g cm^{-3} in (c). Reference values were adjusted for SA-GR at: -0.90 for trees with SA-GR ≤ 0 (green points), 1.03 for trees with 0 < SA-GR ≤ 2 (orange points), and 2.51 for trees with SA-GR > 2 (purple points).

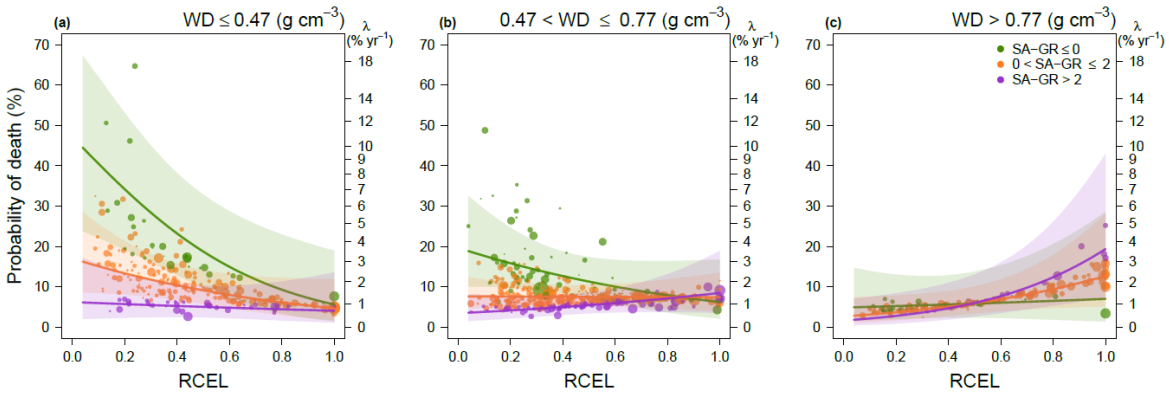

3. Discussion

Tree mortality, a fundamental ecological process determining forest structure and functioning (Franklin *et al.*, 1987), depends on multiple factors that operate at different levels. We studied the role of tree- and species-level factors on the mortality of canopy trees of the Amacayacu Forest Dynamics Plot (AFDP), northwestern Amazon, between 2013 and 2019. We found that the relative crown exposure to light (RCEL), the species-adjusted growth rate (SA-GR), and the species wood density (WD) had a significant influence on canopy tree mortality. While WD and SA-GR were consistently negatively related to tree mortality, the effect of RCEL varied depending on the species' wood density. Our results indicate the importance of the inclusion of plant functional types related to life history strategies (e.g., proxied by wood density) to better predict forest demography under ongoing global changes.

3.1 Influence of tree-level and species-level factors on canopy tree mortality

Overall, WD and SA-GR were consistently negatively related to canopy tree mortality in the AFDP. Canopy trees of species with low wood density were more prone to die than trees with high wood density, a general pattern found across tropical forests (Nascimento *et al.*, 2005; Poorter *et al.*, 2008; Arellano *et al.*, 2019; Aleixo *et al.*, 2019; Reis *et al.*, 2022; Bauman *et al.*, 2022). The high survival of species with high wood density is achieved via higher resistance to pathogen attack (Augspurger & Kelly, 1984), reduced vulnerability to drought-induced hydraulic failure (Hacke *et al.*, 2001; Oliveira *et al.*, 2019), higher tree mechanical stability (Poorter *et al.*, 2008), and less susceptibility to crown damage (Arellano *et al.*, 2019). The high mechanical stability provided by dense wood may be particularly critical for trees in the canopy layer, which are more prone to be disturbed by strong winds

and storms and have higher probability of being directly struck by lightning compared to trees in the understory (Yanoviak *et al.*, 2020; Gora & Esquivel-Muelbert, 2021).

Trees that grew less than their species average (negative SA-GR) had higher probability of death than trees that grew more than their species average (positive SA-GR). This effect was also found by Arellano *et al.*, (2019) for trees with DBH≥10 cm in the Lambir forest dynamics plot in tropical Asia, using a similar species-adjusted standardization of individual growth. Other studies have found that trees with low, near-zero growth rates, were more prone to die than trees with higher growth rates (Rüger *et al.*, 2011; Camac *et al.*, 2018; Esquivel-Muelbert *et al.*, 2020). These results support the idea of employing tree growth rates, relative to conspecifics, as a proxy of the health status of individual trees. Unhealthy trees tend to grow more slowly and have low carbon budgets (Rüger *et al.*, 2011; Camac *et al.*, 2018), which, in turn, reduces trees' ability to tolerate stress and ultimately survive. The extent to which a slow growth rate is the cause or a consequence of a process killing the trees is yet to be determined.

Contrary to our general expectation, we did not find a consistently negative effect of our metric of relative crown exposure to light on canopy tree mortality. However, the probability of death was significantly dependent on the interaction between the relative crown exposure to light and the species' wood density. The relationship between canopy tree mortality and RCEL was negative for trees with low WD and positive for trees with high WD. Since species with low and high wood densities are generally light-demanding and shade-tolerant species, respectively, these results can be explained by differences in the response of these life history strategies to the gradient of relative crown exposure to light (Nascimento *et al.*, 2005; Poorter *et al.*, 2008; Wright *et al.*, 2010; Rüger *et al.*, 2012). The decreasing probability of death for trees with low WD with increasing RCEL indicates that these resource-acquisitive, fast-growing species benefit from being more exposed to sunlight. Fast-growing, low wood density trees require high light conditions to compensate for their high maintenance costs (Givnish, 1988; Lüttge, 2008) and, therefore, have higher probability of death when they are light-limited. In addition, this light-dependent survival of trees with low WD was particularly pronounced for trees growing less than their species

average (i.e., negative SA-GR), but all trees with low WD, regardless their SA-GR, converged toward low probabilities of death when their crowns were fully exposed to sunlight. Light-demanding species with low wood density have been shown to have more positive growth responses to light availability compared to species with higher wood density (Rüger *et al.*, 2012; Cifuentes & Moreno, 2022), which is in line with the sharp decrease of the probability of death with increasing light exposure in low wood density trees.

On the contrary, for high wood density trees, we found a slight increase in the probability of death with increasing relative crown exposure to light. One reason may be that shade-tolerant understory species in this group may have experienced abrupt increases in light availability caused by new gap openings, which increased their risk of mortality due to the exposure to photosynthetically active radiation high above the light saturation point, leading to high leaf stress and photoinhibition (Valladares & Niinemets 2008; but see Cifuentes & Moreno 2022). However, we only found two dead individuals of known understory, shade-tolerant species (*Hirtella racemosa* and *Moquilea jaramilloi*, Chrysobalanaceae) out of 16 dead trees in this high wood density group. Most of the dead trees in this group make up the canopy layer of *terra firme* forests in the Northwestern Amazon (e.g., Eschweilera genus, *Brosimum guianense*, *Licania micrantha*, *Pouteria hispida*) and are expected to tolerate high exposure to light. Therefore, other unmeasured factors (e.g., droughts (Bennett *et al.*, 2015), higher temperatures, lower humidity, higher evaporative demands (Bin *et al.*, 2022), structural damage (Zuleta *et al.*, 2022a)) are more likely to have contributed to the increase in mortality of these high wood density trees with increasing RCEL. Considering the low number of dead trees of high wood density species (6.9%) compared to trees of intermediate (10.1%) and low wood density species (13.8%) (Figure 2-1a), conclusions on the mortality mechanisms of trees with high wood density should be taken with caution (McMahon *et al.*, 2019).

3.2 RCEL as an ecological metric related to tree survival

Although light varies along a continuum across forest strata, the vast majority of studies use a categorical index to characterize the light availability of trees (e.g., crown illumination index; (Clark & Clark, 1992), adapted from Dawkins & Field (1978)). We used a continuous

metric for light availability that accounts for the proportion of total tree crown area that is exposed to vertical sunlight (RCEL) and reflects the amount of resources allocated to the crown that are potentially intercepting direct light. Given that the crown holds the machinery for capturing and transforming light into resources for growth and tree maintenance (Givnish, 1988), RCEL could also be interpreted as a proxy for tree health. A RCEL value lower than one indicates that a portion of the crown area is not observed from above, which may be influenced by at least two non-mutually exclusive mechanisms: crown shading and crown damage. Synchronized ground-based assessments of tree damage and remote sensing-based assessments of tree crowns would be needed to disentangle these mechanisms.

Since crown area is inherently correlated to tree diameter, an obvious question is if RCEL relates to DBH and to what extent are these variables related to tree survival. In our modeling results, the second model with the lowest AICc included DBH instead of RCEL (Table 2-1) and predictions of probability of death based on the model with DBH were similar to predictions from the model including RCEL (Figure S13). However, the correlation between RCEL and DBH was relatively low (Figure S14; R^2 = 4.29%, P<0.001 in standard major axis regression analysis), indicating that both tree-level variables may reflect different mechanisms. While RCEL is associated with the actual exposure of the tree to direct light (as discussed above), DBH is primarily a metric for trunk size. Deviations between RCEL and DBH may be due to tree architecture, crown plasticity, tree light competition, forest gaps, and tree damage (Jucker et al., 2015; Zuleta et al., 2022b). For example, a tree with 10 cm of DBH can be either fully exposed to light, shaded by other trees, or highly damaged. This is very likely the reason why the best model explaining tree survival of canopy trees in our study included RCEL instead of DBH. It is worth nothing, however, that RCEL does not capture the full spectrum of tree light interception along the vertical forest strata (Lüttge, 2008; Bin et al., 2022).

3.3 Implications with climate change

Diverse studies had documented and predicted an increment in the vapor pressure deficit (VPD), air temperature and drought occurrences at the tropical regions (Trenberth *et al.*, 2014; McDowell *et al.*, 2022). As these abiotic factors tend to increase or be more recurrent,

it is expected that larger trees and species of low wood density would be at higher risk of death (Bennett *et al.*, 2015; Zuleta *et al.*, 2017), leading to a decrease in the carbon stocks (principally due to the higher death of large trees), shorter forests stands and probably a more dominance of high wood density species (Aleixo *et al.*, 2019; McDowell *et al.*, 2020). The high probability of death of large trees would lead to a shorter and more dynamic canopy; with higher rates of gap formations and with small trees more prone to occupy the canopy layer, which would ultimately favor the survival of low wood density species at this forest stratum. Also, as VPD and air temperature tend to increase, we would expect less cloud cover and therefore, the relative crown exposure to light would have a bigger impact in the survival of canopy trees, again benefiting the low wooded trees that are more sun exposed. Studies had also documented and projected an increase in the atmospheric CO_2, which allows plants to be more water-efficient in photosynthesis and therefore growth faster (i.e., "CO_2 fertilization"; McDowell *et al.*, 2022). However, the increase in other limiting factors such as poor nutrients and water stress could potentially limit trees to effectively reach faster growth rates (Peñuelas *et al.*, 2017). Irrespective of the pace of climate change, we expect that trees growing more than the species average would have more survival, since this reflects the ability to acquire more resources that could potentially reduce their risk of death.

Overall, it's difficult to define a single path of how climate change will affect tree's survival and moreover predict with certainty the impacts on carbon dynamics and forest composition (Esquivel-Muelbert *et al.*, 2019; Aleixo *et al.*, 2019). Climate change integrates gradual climate trends (e.g., increments in VPD and air temperature) and extreme weather events (e.g., droughts, extreme rainfall periods; Harris *et al.*, 2018), which means that trees experience antagonistic drivers simultaneously or spaced in short periods of time. Moreover, although compositional changes have been observed as climate change progresses, there is a lag between the species response and the velocity of climate change (Esquivel-Muelbert *et al.*, 2019; Feeley *et al.*, 2020). The present study assessed the influence at some tree- and species-levels factors in the mortality of canopy trees at a *terra firme* forest in the northwestern Amazon; it represents a small but valuable step to deepen into the complex tree mortality process. More research is needed about the factors that

influence tree mortality and how they vary with climatic and other potential drivers (e.g., drought, pests, land use change).

4. Conclusion

Our results indicate the importance of accounting for life-history strategies (proxied by wood density) when modeling tropical tree mortality. The survival of trees of species with low wood density depended on both having large proportions of their crowns exposed to vertical sunlight and growing more than their species average. On the contrary, the survival of trees with high wood density decreased with increasing relative crown exposure to light. Moreover, our study integrated high resolution remote sensing with ground-based data, an approach that could be upscaled to evaluate much larger areas. The fast-development and increasing accessibility of remote sensing products constitute a promising tool to better quantify the influence of climatic drivers (e.g., increasing vapor pressure deficit, high winds) on tree mortality as well as the tree- and species-level factors that mediate these responses (e.g., RCEL) at large spatial scales.

A. Supporting information

Table S1. Parameter estimates and statistics for the linear mixed-effects model employed to estimate crown area as a function of DBH in the Amacayacu Forest Dynamics Plot, northwestern Amazon. CI: confidence interval of the estimate. σ^2: residual variance. T_{00}: variance of the species random intercept. T_{11}: variance of the DBH random slope per species. P_{01}: correlation between species random intercepts and slopes.

Predictors	***Estimates***	***CI***	***p***
(Intercept)	-0.03	-0.31 – 0.25	0.835
DBH [log]	1.23	1.15 – 1.32	**<0.001**
Random Effects			
σ^2		0.45	
$T_{00\ species}$		0.59	
$T_{11\ species.log(DBH)}$		0.03	
$\rho_{01\ species}$		-1.00	
$N_{\ species}$		148	
Observations	622		
Marginal R^2 / Conditional R^2	0.756 / NA		
RSE	0.41		

Table S2. Pearson's rank correlation coefficients for all variables initially considered as covariates of canopy tree mortality in the Amacayacu Forest Dynamics Plot, northwestern Amazon. Relative crown exposure to light (RCEL, unitless), log-transformed size (log(DBH), cm), wood density (WD, g cm^{-3}), species-adjusted growth rate (SA-GR, unitless), log-transformed sun-exposed crown area (log(ECA), m^2), log-transformed crown area (log(CA), m^2) and tree growth rate (GR, cm yr^{-1}). * Indicates significant Pearson correlation at 95% confidence (*i.e.,* p-values ≤ 0.05).

	RCEL	**log(DBH)**	**WD**	**SA-GR**	**log(ECA)**	**log(CA)**	**GR**
RCEL	1.00						
log(DBH)	0.18*	1.00					
WD	0.01	-0.08*	1.00				
SA-GR	0.20*	0.04	-0.04	1.00			
log(ECA)	0.76*	0.74*	-0.04	0.17*	1.00		
log(CA)	0.18*	1.00*	-0.08*	0.04	0.74*	1.00	
GR	0.27*	0.09*	-0.26*	0.87*	0.25*	0.09	1.00

Table S3. Summary statistics for tree- and species-level factors obtained from the 984 canopy trees that were crown delimited in the Amacayacu Forest Dynamics Plot, northwestern Amazon. Tree size (DBH, cm), sun-exposed crown area (ECA, m^2), relative crown exposure to light (RCEL, unitless), wood density (WD, g cm^{-3}), species-adjusted growth rate (SA-GR, unitless) and tree growth rate (GR, cm yr^{-1}). Note that ECA, CA, and GR were included here to show their summary statistics but were not included as covariates on the canopy tree mortality models.

Variable	**Min**	**Median**	**Max**	**Mean**	**SD**
DBH (cm)	10.73	33.94	138.84	36.45	16.19
RCEL	0.04	0.42	1.00	0.46	0.24
ECA (m^2)	2.45	33.95	460.87	53.59	57.67
CA (m^2)	21.54	92.16	473.72	103.25	56.97
WD (g cm^{-3})	0.20	0.59	1.05	0.61	0.16
SA-GR	-4.19	1.08	4.25	1.01	1.11
GR (cm yr^{-1})	-0.69	0.41	3.74	0.55	0.55

Table S4. Parameter estimates and statistics for the best generalized linear mixed-effects canopy tree mortality model in the Amacayacu Forest Dynamics Plot, northwestern Amazon. Relative crown exposure to light (RCEL, unitless), wood density (WD, g cm^{-3}), and species-adjusted growth rate (SA-GR, unitless). CI: confidence interval of the estimate. σ^2: residual variance. T_{00}: variance of the species random intercept. ICC: Interclass correlation coefficient.

Predictors	***Log-Odds***	***CI***	***p***
(Intercept)	1.60	-0.37 – 3.58	0.112
RCEL	-5.13	-8.76 – -1.50	**0.006**
WD	-5.86	-9.23 – -2.49	**0.001**
SA-GR	-1.19	-2.18 – -0.20	**0.019**
RCEL * WD	7.36	1.41 – 13.31	**0.015**
RCEL * SA-GR	0.66	-0.08 – 1.40	0.079
WD * SA-GR	1.05	-0.46 – 2.55	0.174
Random Effects			
σ^2	3.29		
$\tau_{00\ species}$	0.73		
ICC	0.18		
$N_{\ species}$	265		
Observations	984		
Marginal R^2 / Conditional R^2	0.062 / 0.232		

Figure S1. Density distribution and skewness for the modulus-transformed tree growth rates using different Θ parameters (*see Methods*) for trees with DBH≥ 1 cm in the Amacayacu Forest Dynamics Plot during the first census interval (2007–2013, 89,322 stems).

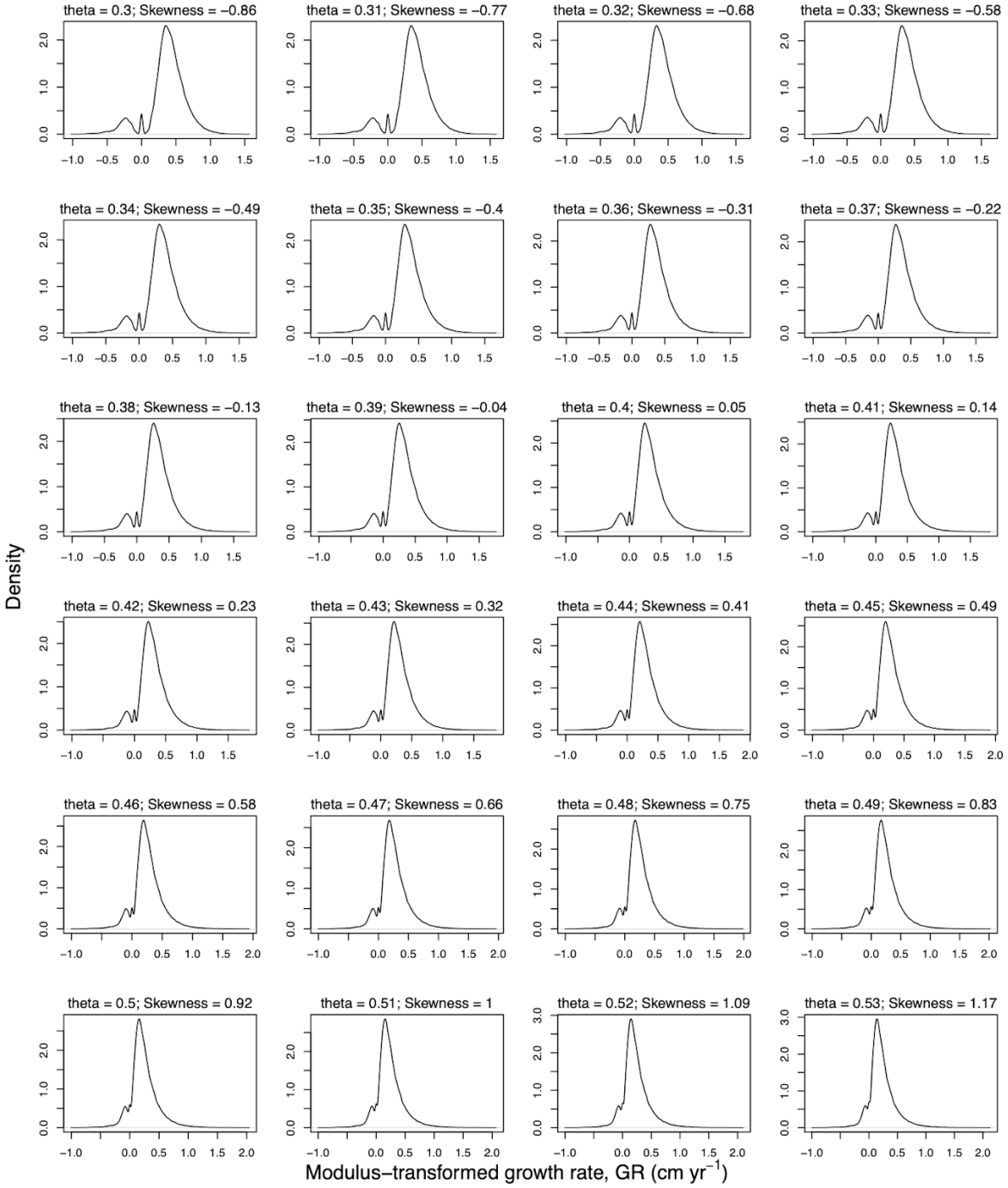

Figure S2. Density distribution and skewness for the modulus-transformed tree growth rates using different Θ parameters (*see Methods*) for trees with DBH≥ 1 cm in the Amacayacu Forest Dynamics Plot during the second census interval (2013–2019, 85,637 stems).

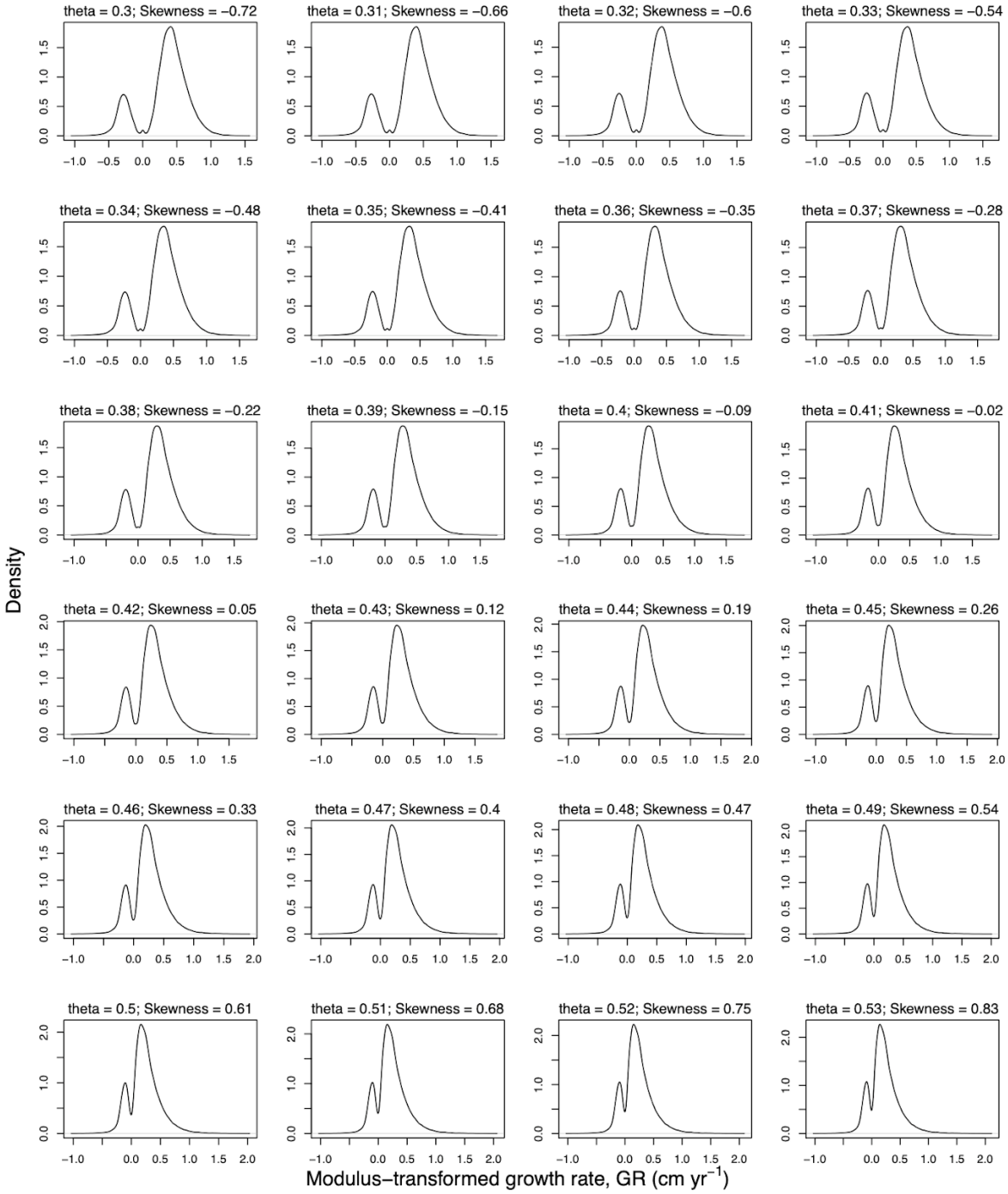

Figure S3. Density distribution and skewness for tree growth rates (*g*, cm yr^{-1}) and the modulus-transformed growth rates with parameter Θ = 0.4 (GR, cm yr^{-1}, *see Methods*) during (a) the first census interval (2007–2013, 89,322 stems) and (b) the second census interval (2013–2019, 85,637 tree stems) for trees with DBH≥ 1 cm in the Amacayacu Forest Dynamics Plot, northwestern Amazon.

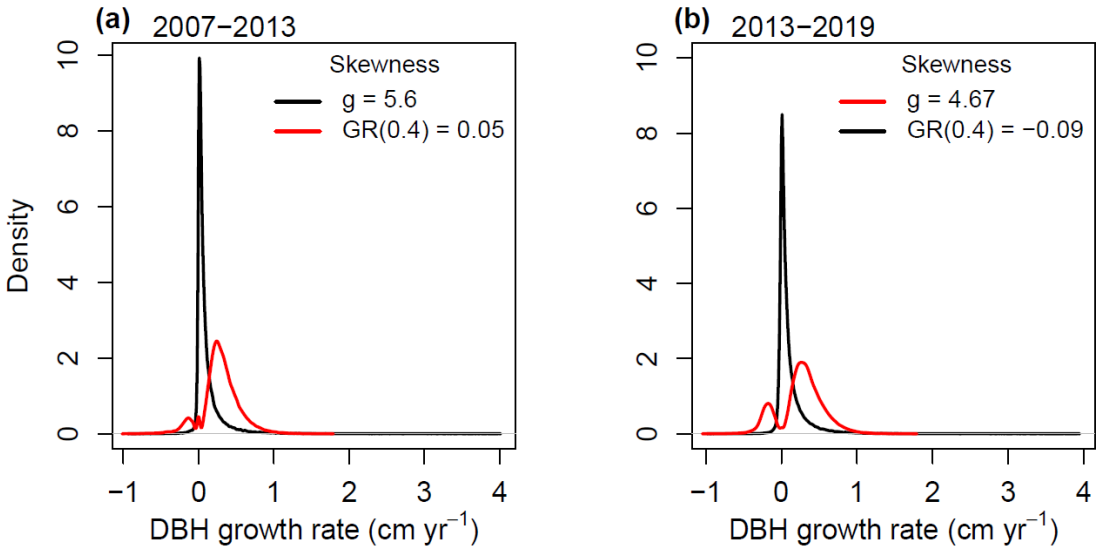

Figure S4. Relationships between tree size (DBH) and three metrics of growth rates for trees with DBH≥ 1 cm during the first census interval (2007-2013, 89,322 stems) in the Amacayacu Forest Dynamics Plot. (a) Growth rate (*g*, cm yr^{-1}), (b) modulus-transformed growth rate with parameter Θ = 0.4 (GR, cm yr^{-1}), and (c) relative growth rate (RGR, cm yr^{-1}). Red points indicate the 984 canopy trees in our sample.

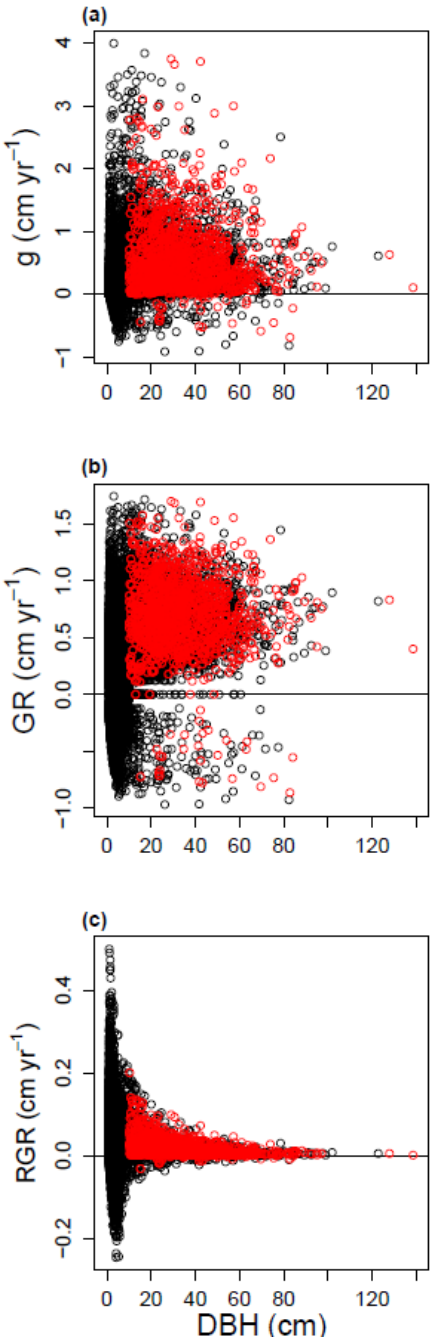

Figure S5. Observed values and model fit for the linear mixed-effects model employed to estimate crown area as a function of DBH in the Amacayacu Forest Dynamics Plot, northwestern Amazon. Points correspond to the observed values of crown area (CA, m^2) at a given tree size (DBH, cm). Red line corresponds to the averaged-population model and shaded areas indicate the 95% confidence interval. Parameter estimates and statistics are presented in Table S1.

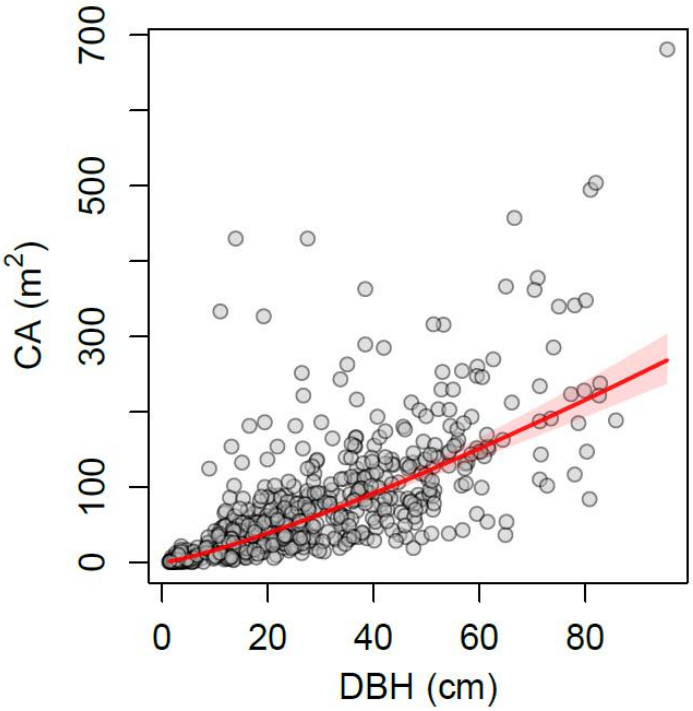

Figure S6. Residual diagnostics for the linear mixed-effects model employed to estimate crown area as a function of DBH in the Amacayacu Forest Dynamics Plot, northwestern Amazon. (a) Quantile-quantile plot of simulated residuals with tests for correct distribution (KS test), dispersion and outliers. (b) Simulated residuals against the predicted value. Note that in (a) the outlier test was significant, meaning that simulated residuals were outside the predicted range (red asterisks on (b)). After a careful inspection of these statistical outliers in the crown survey dataset, we decided to maintain these points.

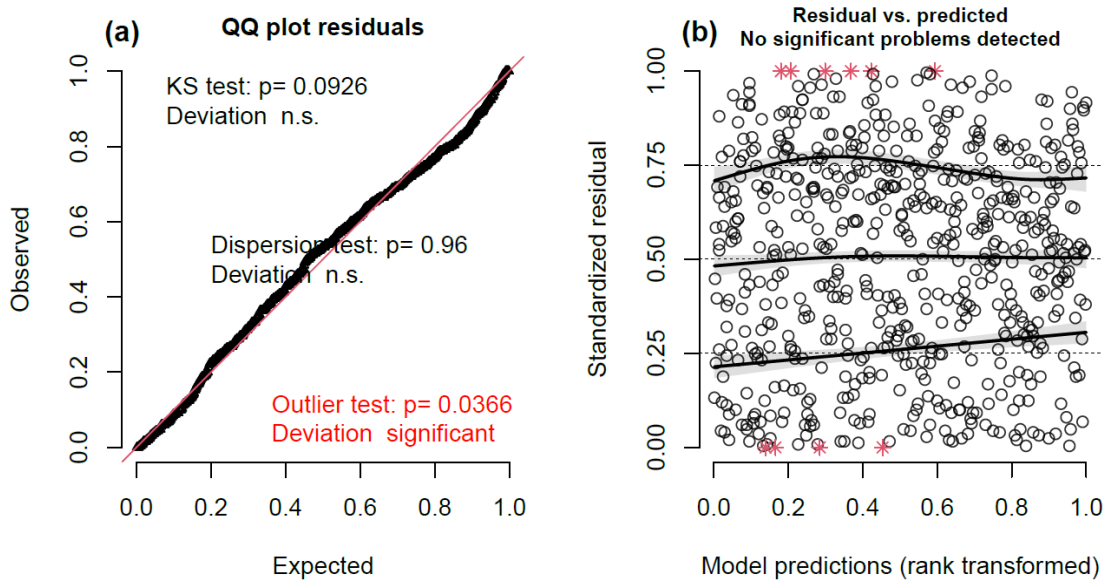

Figure S7. Near-infrared (NIR) image with the survival status of trees studied in 2019 in the Amacayacu Forest Dynamics Plot (AFDP), northwestern Amazon. Delimited crowns for 984 canopy trees of 265 species (48 families) in 18 out of the 25 ha AFDP. Green and blue polygons indicate trees that were found alive (883 trees) and dead (101 trees) in 2019, respectively. Black lines indicate 20 m x 20 m quadrats. The NIR image was obtained using a Remotely Piloted Aircraft System (RPAS) in December 2013.

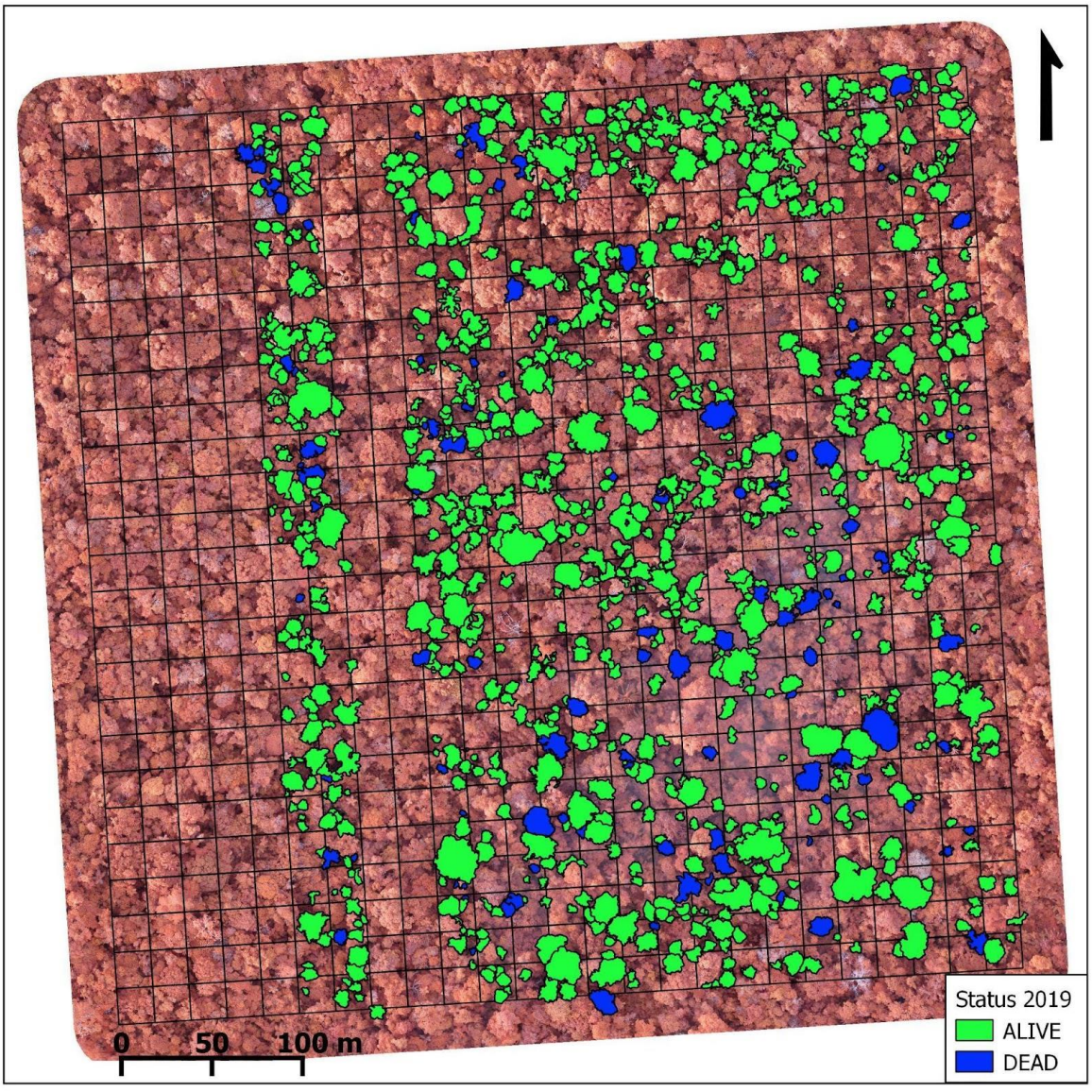

Figure S8. Frequency distribution of variables used in this study. (a) Tree size (DBH, cm), (b) relative crown exposure to light (RCEL, unitless), (c) sun-exposed crown area (ECA, m^2), (d) crown area (CA, m^2), (e) species-adjusted growth rate (SA-GR, unitless), (f) modulus-transformed growth rate (GR, cm yr^{-1}). and (g) species' wood density (WD, g cm^{-3}).

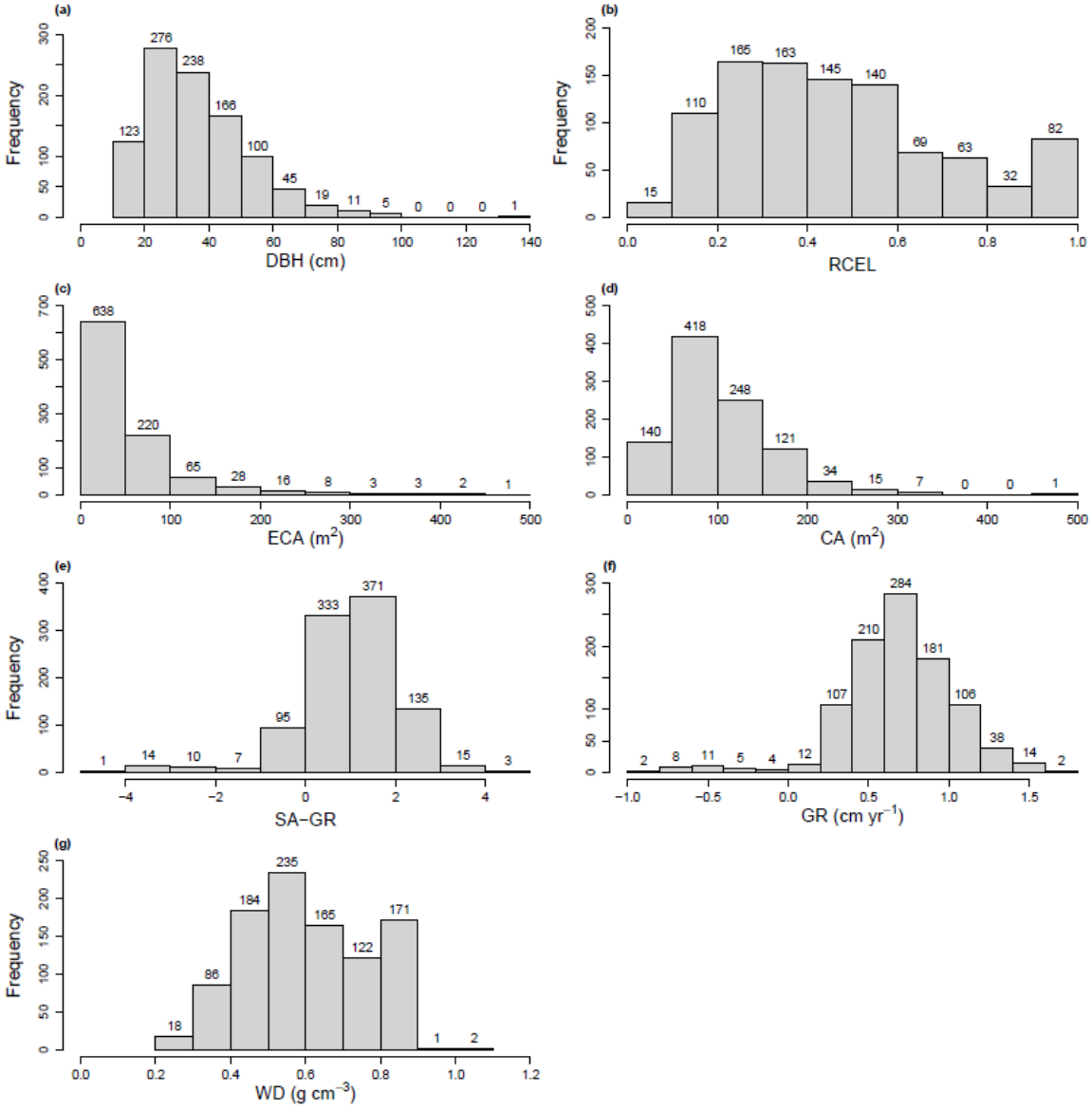

Figure S9. Residual diagnostics for the best generalized linear mixed-effects mortality model in the Amacayacu Forest Dynamics Plot, northwestern Amazon. (a) Quantile-quantile plot of simulated residuals with tests for correct distribution (KS test), dispersion and outliers. (b) Simulated residuals against the predicted value.

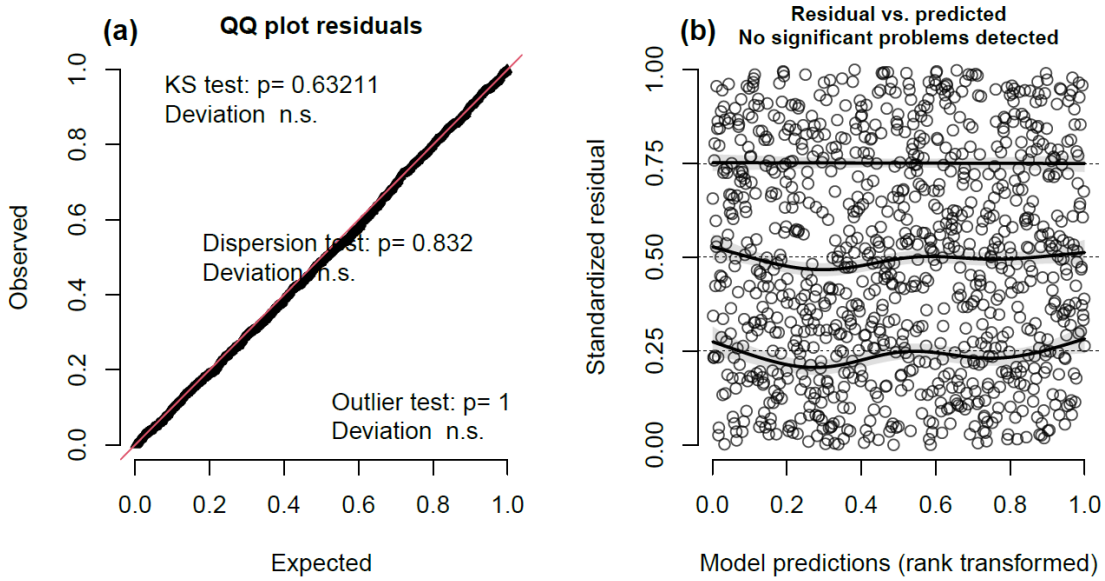

Figure S10. Near-infrared (NIR) image with the predicted probability of death (from the best GLMM model) of crowns delimited in the Amacayacu Forest Dynamics Plot (AFDP), northwestern Amazon. Delimited crowns for 984 canopy trees of 265 species (48 families) in 18 out of the 25 ha AFDP. The color scale indicates the predicted probability of death. Black lines indicate 20 m x 20 m quadrats. The NIR image was obtained using a Remotely Piloted Aircraft System (RPAS) in December 2013.

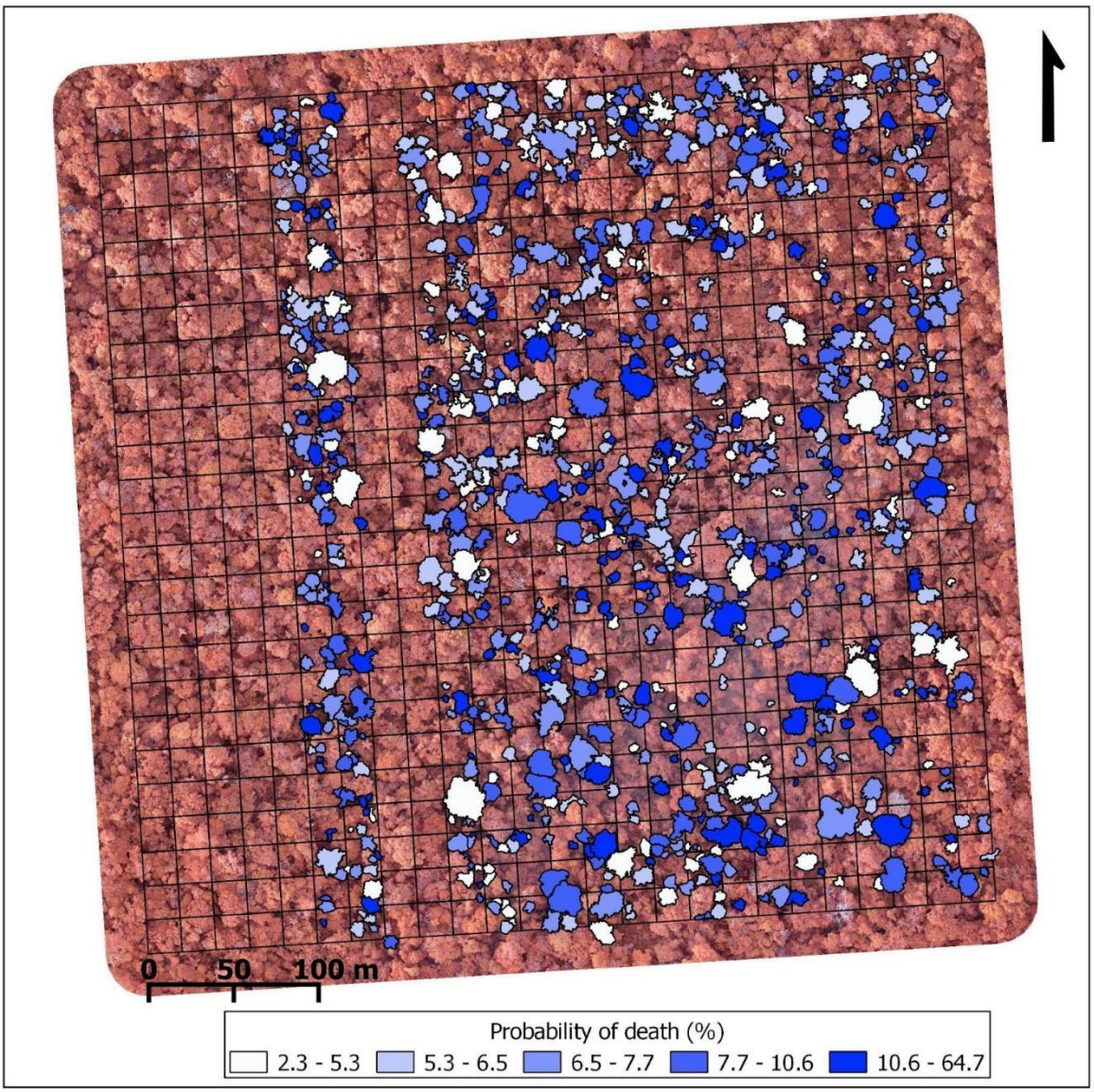

Figure S11. Empirical semi-variogram of the residuals of the best GLMM canopy tree mortality model. Points indicate the semivariance of each bin. Envelopes (dashed lines) correspond to the 95% confidence intervals obtained from Monte Carlo simulations.

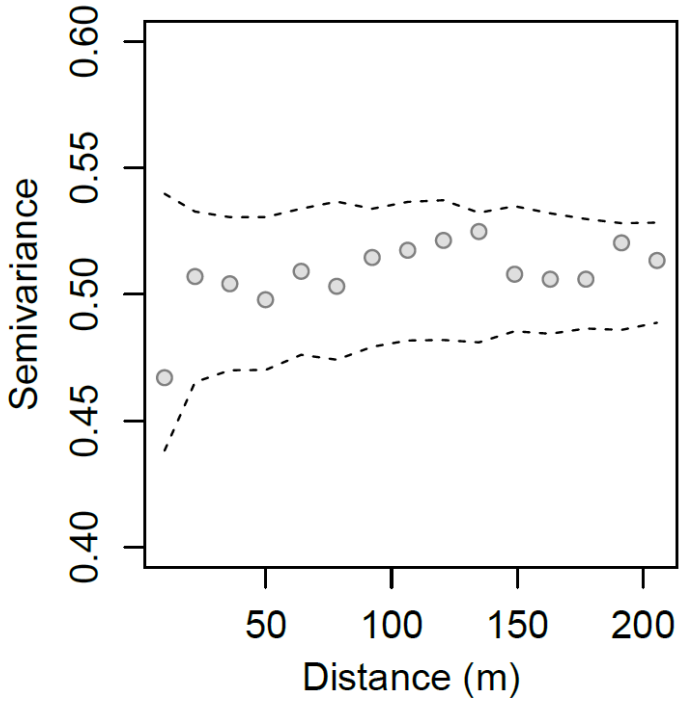

Figure S12. Predicted probability of death for canopy trees in the Amacayacu Forest Dynamics Plot as a function of relative crown exposure to light (RCEL) within different classes of: (a) wood density (WD, g cm^{-3}) and (b) species-adjusted growth rate (SA-GR, unitless). Lines represent the adjusted predictions from the model when conditioned on reference values and shaded areas indicate the 95% confidence interval. Colors of points in (a) indicate WD classes and reference values were adjusted at SA-GR = 1.01 with: WD = 0.41 g cm^{-3} (red), WD = 0.60 g cm^{-3} (blue) and WD = 0.83 g cm^{-3} (green). Colors of points in (b) indicate SA-GR classes and reference values were adjusted at WD = 0.61 g cm^{-3} with: SA-GR = -0.90 (green), SA-GR = 1.03 (orange) and SA-GR = 2.51 (purple). The points size is scaled according to the DBH of the canopy trees. The second vertical axis, λ, corresponds to the annual mortality rate (% yr^{-1}) for the predicted probability of death.

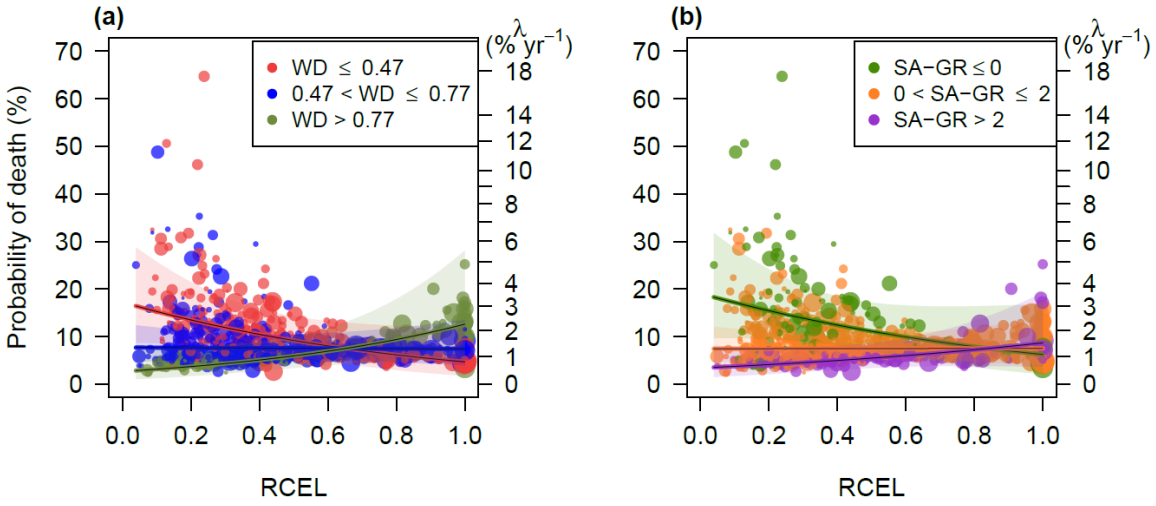

Figure S13. Predicted probability of death (%) for canopy trees in the Amacayacu Forest Dynamics Plot for the second best model as a function of log-transformed size (log(DBH), cm) for three classes of wood density (WD, panels) within three classes of species-adjusted growth rate (SA-GR, color points). Lines represent the adjusted predictions from the model conditioned to reference values and shaded areas indicate the 95% confidence interval. Reference values were adjusted for WD at 0.41 g cm^{-3} in (a), 0.60 g cm^{-3} in (b) and 0.83 g cm^{-3} in (c). Reference values were adjusted for SA-GR at: -0.90 for trees with SA-GR ≤ 0 (green points), 1.03 for trees with 0 < SA-GR ≤ 2 (orange points), and 2.51 for trees with SA-GR > 2 (purple points). The second vertical axis, λ, shows the corresponding annual mortality rate (% yr^{-1}) for the predicted probability of death in a 6-year period.

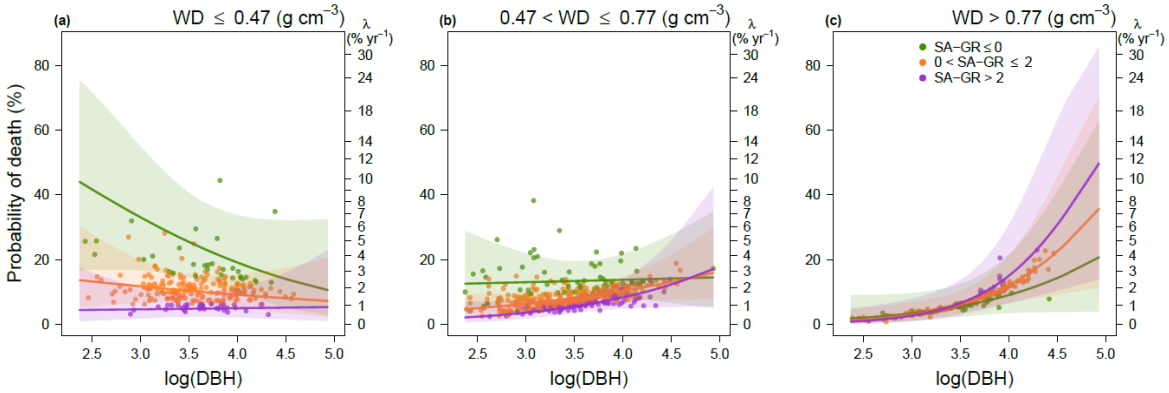

Figure S14. Relationship between log-transformed size and (a) relative crown exposure to light (RCEL, unitless) and (b) log-transformed sun-exposed crown area (log(ECA), m^2). P-values and R-squared values correspond to standard major axis regressions.

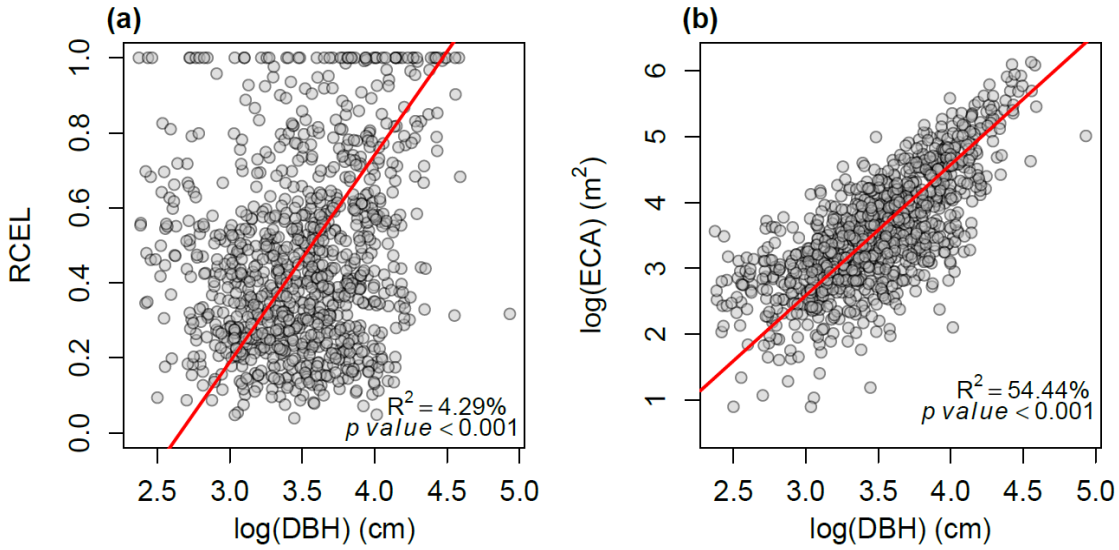

Bibliography

Aleixo I, Norris D, Hemerik L, Barbosa A, Prata E, Costa F, Poorter L. **2019**. Amazonian rainforest tree mortality driven by climate and functional traits. *Nature Climate Change* **9**: 384–388.

Araujo RF, Chambers JQ, Celes CHS, Muller-Landau HC, Santos APF dos, Emmert F, Ribeiro GHPM, Gimenez BO, Lima AJN, Campos MAA, *et al.* 2020. Integrating high resolution drone imagery and forest inventory to distinguish canopy and understory trees and quantify their contributions to forest structure and dynamics (J Müllerová, Ed.). *PLoS ONE* **15**: e0243079.

Araujo RF, Grubinger S, Celes CHS, Negrón-Juárez RI, Garcia M, Dandois JP, Muller-Landau HC. **2021**. Strong temporal variation in treefall and branchfall rates in a tropical forest is related to extreme rainfall: results from 5 years of monthly drone data for a 50\,ha plot. *Biogeosciences* **18**: 6517–6531.

Arellano G, Medina NG, Tan S, Mohamad M, Davies SJ. **2019**. Crown damage and the mortality of tropical trees. *New Phytologist* **221**: 169–179.

Augspurger CK, Kelly CK. **1984**. Pathogen mortality of tropical tree seedlings: experimental studies of the effects of dispersal distance, seedling density, and light conditions. *Oecologia* **61**: 211–217.

Barton K. **2022**. MuMIn: Multi-Model Inference.

Bates D, Mächler M, Bolker B, Walker S. **2015**. Fitting Linear Mixed-Effects Models Using lme4. *Journal of Statistical Software* **67**: 1–48.

Bauman D, Fortunel C, Delhaye G, Malhi Y, Cernusak LA, Bentley LP, Rifai SW, Aguirre-Gutiérrez J, Menor IO, Phillips OL, *et al.* 2022. Tropical tree mortality has increased with rising atmospheric water stress. *Nature*.

Bennett AC, McDowell NG, Allen CD, Anderson-Teixeira KJ. **2015**. Larger trees suffer most during drought in forests worldwide. *Nature Plants* **1**: 15139.

Bin Y, Li Y, Russo SE, Cao H, Ni Y, Ye W, Lian J. **2022**. Leaf trait expression varies with tree size and ecological strategy in a subtropical forest. *Functional Ecology* **36**:

1010–1022.

Bohlman SA, O'Brien S. **2006**. Allometry, adult stature and regeneration requirement of 65 tree species on Barro Colorado Island, Panama. *Journal of Tropical Ecology* **22**: 123–136.

Burnham KP, Anderson DR. **2002**. *Model selection and multi- model inference. A practical information-theoretic approach* (KP Burnham and DR Anderson, Eds.). New York, NY: Springer New York, NY.

Camac JS, Condit R, FitzJohn RG, McCalman L, Steinberg D, Westoby M, Wright SJ, Falster DS. **2018**. Partitioning mortality into growth-dependent and growth-independent hazards across 203 tropical tree species. *Proceedings of the National Academy of Sciences* **115**: 12459–12464.

Chamorro C. **1989**. Biología de los suelos del Parque Nacional Natural Amacayacu y zonas adyacentes (Amazonas, Colombia). *Colombia Geográfica* **15**: 45–63.

Chave J, Coomes D, Jansen S, Lewis SL, Swenson NG, Zanne AE. **2009**. Towards a worldwide wood economics spectrum. *Ecology Letters* **12**: 351–366.

Chave J, Muller-Landau HC, Baker TR, Easdale TA, ter Steege H, Webb CO. **2006**. Regional and phylogenetic variation of wood density across 2456 neotropical tree species. *Ecological Applications* **16**: 2356–2367.

Cifuentes L, Moreno F. **2022**. Trait coordination at leaf level explains the resistance to excess light stress in shade-tolerant tropical tree species (M Mencuccini, Ed.). *Tree Physiology* **42**: 1325–1336.

Clark DA, Clark DB. **1992**. Life History Diversity of Canopy and Emergent Trees in a Neotropical Rain Forest. *Ecological Monographs* **62**: 315–344.

Condit R, Aguilar S, Hernandez A, Perez R, Lao S, Angehr G, Hubbell SP, Foster RB. **2004**. Tropical forest dynamics across a rainfall gradient and the impact of an El Niño dry season. *Journal of Tropical Ecology* **20**: 51–72.

Condit R, Pérez R, Lao S, Aguilar S, Hubbell SP. **2017**. Demographic trends and climate over 35 years in the Barro Colorado 50 ha plot. *Forest Ecosystems* **4**: 17.

Cushman KC, Bunyavejchewin S, Cárdenas D, Condit R, Davies SJ, Duque Á, Hubbell SP, Kiratiprayoon S, Lum SKY, Muller-Landau HC. **2021**. Variation in trunk taper of buttressed trees within and among five lowland tropical forests. *Biotropica* **53**: 1442–1453.

Cushman KC, Detto M, García M, Muller-Landau HC. **2022**. Soils and topography

control natural disturbance rates and thereby forest structure in a lowland tropical landscape. *Ecology Letters* **25**: 1126–1138.

Davies SJ, Abiem I, Abu Salim K, Aguilar S, Allen D, Alonso A, Anderson-Teixeira K, Andrade A, Arellano G, Ashton PS, *et al.* 2021. ForestGEO: Understanding forest diversity and dynamics through a global observatory network. *Biological Conservation* **253**: 108907.

Dawkins HC, Field DRB. **1978**. *A long-term surveillance system for british woodland vegetation*. Oxford, United Kingdom: Department of Forestry, Oxford University.

Duque A, Muller-Landau HC, Valencia R, Cardenas D, Davies SJ, de Oliveira A, Pérez ÁJ, Romero-Saltos H, Vicentini A. **2017**. Insights into regional patterns of Amazonian forest structure, diversity, and dominance from three large terra-firme forest dynamics plots. *Biodiversity and Conservation* **26**: 669–686.

Esquivel-Muelbert A, Phillips OL, Brienen RJW, Fauset S, Sullivan MJP, Baker TR, Chao K-J, Feldpausch TR, Gloor E, Higuchi N, *et al.* 2020. Tree mode of death and mortality risk factors across Amazon forests. *Nature Communications* **11**: 5515.

Esquivel-Muelbert A, Baker TR, Dexter KG, Lewis SL, Brienen RJW, Feldpausch TR, Lloyd J, Monteagudo-Mendoza A, Arroyo L, Álvarez-Dávila E, *et al.* 2019. Compositional response of Amazon forests to climate change. *Global Change Biology* **25**: 39–56.

Feeley KJ, Bravo-Avila C, Fadrique B, Perez TM, Zuleta D. **2020**. Climate-driven changes in the composition of New World plant communities. *Nature Climate Change* **10**: 965–970.

Franklin JF, Shugart HH, Harmon ME. **1987**. Tree death as an ecological process. *BioScience* **37**: 550–556.

Friedlingstein P, Jones MW, O'Sullivan M, Andrew RM, Bakker DCE, Hauck J, Le Quéré C, Peters GP, Peters W, Pongratz J, *et al.* 2022. Global Carbon Budget 2021. *Earth System Science Data* **14**: 1917–2005.

Givnish T. **1988**. Adaptation to sun and shade: a whole-plant perspective. *Functional Plant Biology* **15**: 63.

Gora EM, Esquivel-Muelbert A. **2021**. Implications of size-dependent tree mortality for tropical forest carbon dynamics. *Nature Plants* **7**: 384–391.

Grizonnet M, Michel J, Poughon V, Inglada J, Savinaud M, Cresson R. **2017**. Orfeo

ToolBox: open source processing of remote sensing images. *Open Geospatial Data, Software and Standards* **2**: 15.

Hacke UG, Sperry JS, Pockman WT, Davis SD, McCulloh KA. **2001**. Trends in wood density and structure are linked to prevention of xylem implosion by negative pressure. *Oecologia* **126**: 457–461.

Harris RMB, Beaumont LJ, Vance TR, Tozer CR, Remenyi TA, Perkins-Kirkpatrick SE, Mitchell PJ, Nicotra AB, McGregor S, Andrew NR, *et al.* 2018. Biological responses to the press and pulse of climate trends and extreme events. *Nature Climate Change* **8**: 579–587.

Hartig F. **2021**. DHARMa: residual diagnostics for hierarchical (multi-level/mixed) regression models.

Hubau W, Lewis SL, Phillips OL, Affum-Baffoe K, Beeckman H, Cuní-Sanchez A, Daniels AK, Ewango CEN, Fauset S, Mukinzi JM, *et al.* 2020. Asynchronous carbon sink saturation in African and Amazonian tropical forests. *Nature* **579**: 80–87.

Jucker T, Bouriaud O, Coomes DA. **2015**. Crown plasticity enables trees to optimize canopy packing in mixed-species forests (J Baltzer, Ed.). *Functional Ecology* **29**: 1078–1086.

Lüttge U. **2008**. Tropical Forests. I. Physiognomy and Functional Structure. In: Lüttge U, ed. Physiological Ecology of Tropical Plants. Berlin, Heidelberg: Springer Berlin Heidelberg, 51–101.

Lutz JA, Furniss TJ, Johnson DJ, Davies SJ, Allen D, Alonso A, Anderson-Teixeira KJ, Andrade A, Baltzer J, Becker KML, *et al.* 2018. Global importance of large-diameter trees. *Global Ecology and Biogeography* **27**: 849–864.

Martínez-Cano I, Muller-Landau HC, Joseph Wright S, Bohlman SA, Pacala SW. **2019**. Tropical tree height and crown allometries for the Barro Colorado Nature Monument, Panama: A comparison of alternative hierarchical models incorporating interspecific variation in relation to life history traits. *Biogeosciences* **16**: 847–862.

Mazerolle M. **2020**. AICcmodavg: Model selection and multimodel inference based on (Q)AIC(c).

McDowell NG, Allen CD, Anderson-Teixeira K, Aukema BH, Bond-Lamberty B, Chini L, Clark JS, Dietze M, Grossiord C, Hanbury-Brown A, *et al.* 2020. Pervasive shifts in forest dynamics in a changing world. *Science* **368**.

McDowell NG, Sapes G, Pivovaroff A, Adams HD, Allen CD, Anderegg WRL, Arend

M, Breshears DD, Brodribb T, Choat B, *et al.* 2022. Mechanisms of woody-plant mortality under rising drought, CO2 and vapour pressure deficit. *Nature Reviews Earth & Environment* **3**: 294–308.

McMahon SM, Arellano G, Davies SJ. **2019**. The importance and challenges of detecting changes in forest mortality rates. *Ecosphere* **10**: e02615.

Metcalf CJE, Clark JS, Clark DA. **2009**. Tree growth inference and prediction when the point of measurement changes: modelling around buttresses in tropical forests. *Journal of Tropical Ecology* **25**: 1–12.

Muller-Landau HC, Condit RS, Chave J, Thomas SC, Bohlman SA, Bunyavejchewin S, Davies S, Foster R, Gunatilleke S, Gunatilleke N, *et al.* 2006. Testing metabolic ecology theory for allometric scaling of tree size, growth and mortality in tropical forests. *Ecology Letters* **9**: 575–588.

Nakagawa S, Schielzeth H. **2013**. A general and simple method for obtaining R2 from generalized linear mixed-effects models (RB O'Hara, Ed.). *Methods in Ecology and Evolution* **4**: 133–142.

Nascimento HEM, Laurance WF, Condit R, Laurance SG, D'Angelo S, Andrade AC. **2005**. Demographic and life-history correlates for Amazonian trees. *Journal of Vegetation Science* **16**: 625–634.

Negrón-Juárez R, Jenkins H, Raupp C, Riley W, Kueppers L, Magnabosco Marra D, Ribeiro G, Monteiro M, Candido L, Chambers J, *et al.* 2017. Windthrow variability in Central Amazonia. *Atmosphere* **8**: 28.

Oliveira RS, Costa FRC, Baalen E, Jonge A, Bittencourt PR, Almanza Y, Barros F de V, Cordoba EC, Fagundes M V, Garcia S, *et al.* 2019. Embolism resistance drives the distribution of Amazonian rainforest tree species along hydro-topographic gradients. *New Phytologist* **221**: 1457–1465.

Peñuelas J, Ciais P, Canadell JG, Janssens IA, Fernández-Martínez M, Carnicer J, Obersteiner M, Piao S, Vautard R, Sardans J. **2017**. Shifting from a fertilization-dominated to a warming-dominated period. *Nature Ecology and Evolution* **1**: 1438–1445.

Piponiot C, Anderson-Teixeira KJ, Davies SJ, Allen D, Bourg NA, Burslem DFRP, Cárdenas D, Chang-Yang C, Chuyong G, Cordell S, *et al.* 2022. Distribution of biomass dynamics in relation to tree size in forests across the world. *New Phytologist* **234**: 1664–1677.

Poorter L, Wright SJ, Paz H, Ackerly DD, Condit R, Ibarra-Manríquez G, Harms KE, Licona JC, Martínez-Ramos M, Mazer SJ, *et al.* 2008. Are functional traits good predictors of demographic rates? Evidence from five neotropical forests. *Ecology* **89**: 1908–1920.

QGIS Geographic Information System. **2022**. QGIS.

R Core Team. **2021**. R: a language and environment for statistical computing.

Reis SM, Marimon BS, Esquivel-Muelbert A, Marimon BH, Morandi PS, Elias F, Oliveira EA, Galbraith D, Feldpausch TR, Menor IO, *et al.* 2022. Climate and crown damage drive tree mortality in southern Amazonian edge forests. *Journal of Ecology* **110**: 876–888.

Rüger N, Huth A, Hubbell SP, Condit R. **2011**. Determinants of mortality across a tropical lowland rainforest community. *Oikos* **120**: 1047–1056.

Rüger N, Wirth C, Wright SJ, Condit R. **2012**. Functional traits explain light and size response of growth rates in tropical tree species. *Ecology* **93**: 2626–2636.

Russo SE, Davies SJ, King DA, Tan S. **2005**. Soil-related performance variation and distributions of tree species in a Bornean rain forest. *Journal of Ecology* **93**: 879–889.

Russo SE, McMahon SM, Detto M, Ledder G, Wright SJ, Condit RS, Davies SJ, Ashton PS, Bunyavejchewin S, Chang-Yang C-H, *et al.* 2021. The interspecific growth–mortality trade-off is not a general framework for tropical forest community structure. *Nature Ecology & Evolution* **5**: 174–183.

Trenberth KE, Dai A, Van Der Schrier G, Jones PD, Barichivich J, Briffa KR, Sheffield J. **2014**. Global warming and changes in drought. *Nature Climate Change* **4**: 17–22.

Valladares F, Niinemets Ü. **2008**. Shade Tolerance, a Key Plant Feature of Complex Nature and Consequences. *Annual Review of Ecology, Evolution, and Systematics* **39**: 237–257.

Wright SJ. **2002**. Plant diversity in tropical forests: A review of mechanisms of species coexistence. *Oecologia* **130**: 1–14.

Wright SJ, Kitajima K, Kraft NJB, Reich PB, Wright IJ, Bunker DE, Condit R, Dalling JW, Davies SJ, Díaz S, *et al.* 2010. Functional traits and the growth–mortality trade-off in tropical trees. *Ecology* **91**: 3664–3674.

Yanoviak SP, Gora EM, Bitzer PM, Burchfield JC, Muller-Landau HC, Detto M, Paton S, Hubbell SP. **2020**. Lightning is a major cause of large tree mortality in a lowland

neotropical forest. *New Phytologist* **225**: 1936–1944.

Zanne AE, López-González G, Coomes DA, Ilic J, Jansen S, Lewis SL, Miller RB, Swenson NG, Wiemann MC, Chave J. **2009**. Global wood density database. *Dryad Digital Repository*.

Zuleta D, Arellano G, Muller-Landau HC, McMahon SM, Aguilar S, Bunyavejchewin S, Cardenas D, Chang-Yang C, Duque A, Mitre D, *et al.* 2022a. Individual tree damage dominates mortality risk factors across six tropical forests. *New Phytologist* **233**: 705–721.

Zuleta D, Duque A, Cardenas D, Muller-Landau HC, Davies SJ. **2017**. Drought-induced mortality patterns and rapid biomass recovery in a terra firme forest in the Colombian Amazon. *Ecology* **98**: 2538–2546.

Zuleta D, Krishna Moorthy SM, Arellano G, Verbeeck H, Davies SJ. **2022b**. Vertical distribution of trunk and crown volume in tropical trees. *Forest Ecology and Management* **508**: 120056.

Zuleta D, Russo SE, Barona A, Barreto-Silva JS, Cardenas D, Castaño N, Davies SJ, Detto M, Sua S, Turner BL, *et al.* 2020. Importance of topography for tree species habitat distributions in a terra firme forest in the Colombian Amazon. *Plant and Soil* **450**: 133–149.